PERGAMON

International Journal of Solids and Structures 40 (2003) 899–940

INTERNATIONAL JOURNAL OF SOLIDS and STRUCTURES

www.elsevier.com/locate/ijsolstr

The three-dimensional steady-state thermo-elastodynamic problem of moving sources over a half space

G. Lykotrafitis [a], H.G. Georgiadis [b,*]

[a] *Graduate Aeronautical Laboratories, Mail Stop 105-50, California Institute of Technology, Pasadena, CA 91125, USA*
[b] *Mechanics Division, National Technical University of Athens, 1 Konitsis Street, Zographou GR-15773, Greece*

Received 18 December 2001; received in revised form 18 October 2002

Abstract

A procedure based on the Radon transform and elements of distribution theory is developed to obtain fundamental thermoelastic three-dimensional (3D) solutions for thermal and/or mechanical point sources moving steadily over the surface of a half space. A concentrated heat flux is taken as the thermal source, whereas the mechanical source consists of normal and tangential concentrated loads. It is assumed that the sources move with a constant velocity along a fixed direction. The solutions obtained are exact within the bounds of Biot's coupled thermo-elastodynamic theory, and results for surface displacements are obtained over the entire speed range (i.e. for sub-Rayleigh, super-Rayleigh/subsonic, transonic and supersonic source speeds). This problem has relevance to situations in Contact Mechanics, Tribology and Dynamic Fracture, and is especially related to the well-known heat checking problem (thermo-mechanical cracking in an unflawed half-space material from high-speed asperity excitations). Our solution technique fully exploits as auxiliary solutions the ones for the corresponding plane-strain and anti-plane shear problems by reducing the original 3D problem to two separate 2D problems. These problems are uncoupled from each other, with the first problem being thermoelastic and the second one pure elastic. In particular, the auxiliary plane-strain problem is completely analogous to the original problem, not only with regard to the field equations but also with regard to the boundary conditions. This makes the technique employed here more advantageous than other techniques, which require the prior determination of a fictitious auxiliary plane-strain problem through solving an integral equation.

Keywords: Thermoelasticity; Elastodynamics; Moving sources; Three-dimensional problems; Rayleigh waves; Radon transform; Distributions

1. Introduction

The *rapid* motion of a point mechanical and/or thermal load over the surface of a half space is a problem that has relevance to situations in Contact Mechanics, Tribology and Dynamic Fracture. Typical cases of application are the following: (i) Motion of an asperity developed on the mating surface of mechanical

* Corresponding author. Tel.: +30-210-7721365; fax: +30-210-7721302.
E-mail address: georgiad@central.ntua.gr (H.G. Georgiadis).

0020-7683/02/$ - see front matter © 2002 Elsevier Science Ltd. All rights reserved.
PII: S0020-7683(02)00613-3

systems that are pressed against each other and undergo relative sliding rapid motion accompanied by dry friction. Such an asperity may be a material inclusion or some thermo-mechanical deformation of the mating surface (see e.g. Ju and Huang, 1982; Barber, 1984; Kennedy, 1984; Huang and Ju, 1985; Barber and Ciavarella, 2000). (ii) Brake systems (see e.g. Ling and Ng, 1962; Huang and Ju, 1985; Barber and Ciavarella, 2000). (iii) Crack face contact in intersonic interfacial rapid fracture of bimaterial plates (see e.g. Rosakis et al., 1998; Huang et al., 1998). (iv) Deformations generated by the motion of high-speed modern trains (Lefeuvemesgouez et al., 2000; Krylov et al., 2000). In the foregoing situations, the moving mechanical/thermal load may produce severe deformation and temperature rises in a thin zone near the contact zone, and therefore may cause excessive wear and even cracking near this zone.

In many cases, the problem described above can be modeled as a *steady-state* situation involving a half space under mechanical/thermal loads, which move over the surface of a half space at a constant velocity. In addition, the solution of the problem with *concentrated* loads may serve as a Green's function for solving, through integral equations, more general contact problems (see, e.g., for 2D elastodynamic and thermo-elastodynamic contact problems the works by Georgiadis and Barber, 1993, and Brock and Georgiadis, 2000). Here, the 3D problem of moving mechanical/thermal point sources is examined within the coupled thermo-elastodynamic theory of Biot (1956). Additional aspects of this theory and solutions to specific problems were presented by, among others, Chadwick (1960), Carlson (1972), Dassios and Grillakis (1984), Massalas et al. (1985), Atkinson and Craster (1992), Brock (1995, 1997), Brock and Georgiadis (1997, 1999), and Georgiadis et al., 1998, 1999).

Existing analyses of thermoelastic problems dealing with moving mechanical/thermal loads over the surface of a half space may be categorized according to the form of the governing equations employed, i.e. one may distinguish treatments which employ *uncoupled* or *coupled* thermoelasticity and also treatments which exclude or include *inertial* (dynamic) effects. For instance, the approaches of Ling and Mow (1965); Jahanshahi (1966); Mow and Cheng (1967); Kilaparti and Burton (1978); Barber (1984), and Bryant (1988) use uncoupled thermoelasticity and exclude inertial effects, whereas the analyses of Ju and Huang (1982), and Huang and Ju (1985) employ uncoupled thermoelasticity but include inertial effects. On the contrary, Brock and Georgiadis (1997, 1999) provide more complete exact solutions that include both thermal-coupling and inertial effects. In addition, the work of Brock et al. (1997) considers transient effects and makes comparisons with the steady-state results of Brock and Georgiadis (1997) revealing that the *steady-state* assumption is indeed satisfactory far away from the point of the first application of the loading, along the half-space surface.

The problem considered here is the 3D analogue of the plane-strain problem considered by Brock and Georgiadis (1997) and it is based on coupled thermo-elastodynamics too. A related study is that of Brock and Rodgers (1997) which, however, was restricted to consider only a normal moving load (the cases of a tangential load and a heat source were not considered) and a sub-Rayleigh load speed. In the present study, we follow a different method than the Laplace transform (double and two-sided) method of Brock and Rodgers (1997) and, more importantly, we obtain results over the *entire* speed range (i.e. for sub-Rayleigh, super-Rayleigh/subsonic, transonic and supersonic speeds of the loads) and for *all* cases of loading (i.e. normal, tangential and thermal loads). Notice also that, with the exception of the work of Brock and Rodgers (1997), all studies in the literature do not consider the 3D case.

In the absence of thermal effects, the present case reduces to the classical 3D steady-state elastodynamic problem of moving point loads along the surface of a half space. This problem was considered by, among others, Eason (1965); Lansing (1966); Barber (1996), and Georgiadis and Lykotrafitis (2001). Since the 'pure mechanical' problem may serve as a guide for the more difficult thermo-mechanical problem considered here, it is interesting to briefly discuss the solution procedures in these studies. Eason (1965) and Lansing (1966) employed double Fourier transforms but, especially when the load speed lies in the super-Rayleigh regime, the double Fourier (or, equivalently, the double two-sided Laplace) transform technique becomes particularly involved.

In our opinion, the approaches of Barber (1996) and Georgiadis and Lykotrafitis (2001) are much simpler than the approaches of Eason (1965) and Lansing (1966). Also, the technique of Georgiadis and Lykotrafitis (2001) fully exploits the existing solution of the corresponding plane-strain problem by treating the latter problem as an auxiliary one. In particular, Georgiadis and Lykotrafitis (2001) developed a technique based on the Radon transform (see e.g. Gel'fand et al., 1966), certain coordinate transformations and distribution theory to reduce the original 3D problem to two auxiliary problems, which are 2D and uncoupled (one problem is of the plane-strain type and the other of the anti-plane shear type). These corresponding problems are *completely* analogous to the original 3D problem, not only with regard to the field equations but also with regard to the boundary conditions. On the other hand, Barber (1996) presented a superposition technique of the Smirnov–Sobolev type (see e.g. Sveklo, 1964; Poruchikov, 1993) for the specific case of a normal load. This reduces the original 3D problem to an auxiliary 2D problem. The auxiliary plane-strain problem now is *not* completely analogous to the original 3D problem and its determination can only be achieved through the solution of an integral equation. In general also, the solution to such an auxiliary problem probably cannot be readily available in the literature since the problem is somewhat artificial, as relative experience indicates (see e.g. Poruchikov, 1993). In view of the above, it seems that the Radon-transform technique (which is not based on explicit superposition-type arguments) is more direct than the Smirnov–Sobolev technique. In addition, Georgiadis and Lykotrafitis (2001) provided a complete solution to the 'pure mechanical' 3D problem, filling therefore a gap in the literature related to this problem, in the sense that they obtained results over the entire speed range (i.e. for sub-Rayleigh, super-Rayleigh/subsonic, transonic and supersonic speeds of the loads) and for both normal and tangential loads.

Here, in considering the 3D problem of moving mechanical/heat point sources, the Radon-transform approach is followed by fully taking advantage of existing solutions of the corresponding 2D problems. The two auxiliary problems involving half-plane domains and surface loadings are again uncoupled; the first is the thermo-elastodynamic plane-strain problem of moving mechanical/thermal line sources (Brock and Georgiadis, 1997) and the second is the 'pure mechanical' anti-plane shear problem of a moving line load (Georgiadis and Lykotrafitis, 2001). After establishing the correspondence principle connecting the 3D problem with the auxiliary ones, the solution to the original problem follows by performing first a coordinate transformation and then taking the inverse Radon transform of the 2D solutions. In the course of the inversions, extensive use of distribution theory is made concerning mainly treatment of products of distributions.

Another comment pertains to the applicability of the Radon-transform approach described above on *non-axisymmetric* situations. In general, the method still works in the case that the loading is not axially symmetric but the 2D auxiliary problems are no longer direct analogues of the original 3D problem. The method is particularly simple when there is no angular dependence in the boundary conditions (as is the case here) *regardless* of possible loss of axisymmetry due to the material response (anisotropy) and/or the generation of Mach waves in the medium (this asymmetry is induced by changes in the nature of governing PDEs of steady-state dynamical problems—the changes being manifested by the existence of different velocity regimes).

Finally, we should also mention that interesting applications of the Radon transform in elasticity problems were presented earlier by Willis (1970, 1973), and more recently by, among others, Wang and Achenbach (1996) and Shmegera (2000).

2. Problem statement

Consider a thermally conducting linearly elastic isotropic body in the form of a 3D half space $x_3 \geqslant 0$. This otherwise unloaded body is initially at rest and at a uniform temperature T_0 (expressed in K), but at time $t = 0$ is disturbed by the motion of a mechanical/thermal source (see Fig. 1). The concentrated point

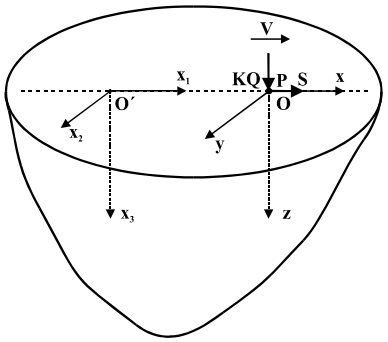

Fig. 1. Thermal and mechanical sources moving under constant velocity V over the surface of an elastic half space. $O'x_1x_2x_3$ is a fixed Cartesian coordinate system and $Oxyz$ is a moving Cartesian coordinate system attached to the loads.

load has components P and S (these loads are in the directions x_3 and x_1, respectively), whereas the point heat source has intensity KQ, with K denoting the thermal conductivity expressed in (power) (length)$^{-1}$ (K)$^{-1}$ and Q being a multiplier expressed in (length) (K). The mechanical/thermal source moves under a constant velocity V over the surface $x_3 = 0$ and along the x_1-direction. Notice that a tangential load in the direction orthogonal to the direction of motion (i.e. along the x_2-direction) is not considered because this case is rather impractical. Indeed, it is difficult for one to apply and maintain a moving tangential load having a direction that is orthogonal to the direction of motion. This case, however, was considered in Georgiadis and Lykotrafitis (2001) for the sake of completeness.

Then, the governing equations of the problem according to the linear coupled thermo-elastodynamic theory (Biot, 1956; Chadwick, 1960; Carlson, 1972) will be written. With respect to a fixed Cartesian coordinate system $O'x_j$ $(j = 1, 2, 3)$, the equations of motion (thermoelastic Navier–Cauchy equations) and the generalized heat-conduction equation, in the absence of body forces and sources, along with the stress–strain relations (Duhamel–Neumann law) are as follows:

$$\mu\nabla^2\mathbf{u} + (\lambda+\mu)\nabla(\nabla\cdot\mathbf{u}) - \kappa_0(3\lambda+2\mu)\nabla\theta = \rho\frac{\partial^2\mathbf{u}}{\partial t^2}, \tag{1a}$$

$$K\nabla^2\theta - \rho C_v\frac{\partial\theta}{\partial t} - \kappa_0(3\lambda+2\mu)T_0\frac{\partial(\nabla\cdot\mathbf{u})}{\partial t} = 0, \tag{1b}$$

$$\boldsymbol{\sigma} = \mu(\nabla\mathbf{u} + \mathbf{u}\nabla) + \lambda(\nabla\cdot\mathbf{u})\mathbf{1} - \kappa_0(3\lambda+2\mu)\theta\mathbf{1}, \tag{1c}$$

where $\mathbf{u}$ is the displacement vector with components u_j, T is the current temperature, $\theta = T - T_0$ is the change in temperature, $\boldsymbol{\sigma}$ is the stress tensor with components σ_{ij} $(i, j = 1, 2, 3)$, $\mathbf{1}$ is the identity tensor, ∇ is the 3D gradient operator, $\nabla\cdot\mathbf{u}$ is the dilatation, ∇^2 is the Laplacian operator, (λ, μ) are the Lamé constants, ρ is the mass density, κ_0 is the coefficient of thermal expansion, and C_v is the specific heat at constant deformation. It is also noticed that the third term in the LHS of Eqs. (1a) and (1b) arises from the interaction of the deformation field with the thermal field. In this process, however, shear (rotational) waves remain unaffected by the ability of the medium to conduct heat; only longitudinal (dilatational) waves are modified by thermal straining and, conversely, only mechanical energy expended in volume changes is converted into heat.

We now introduce the standard *steady-state* assumption (see e.g. Fung, 1965; Georgiadis, 1986; Barber, 1996; Brock and Rodgers, 1997) according to which a steady stress and displacement field is created in the medium w.r.t. an observer situated in a frame of reference attached to the moving load, if this source has been moving steadily for a sufficiently long time. In this way, any transients can reasonably be avoided

(therefore gaining considerable simplification in the analysis) and, moreover, upon introduction of the Galilean transformation

$$x = x_1 - Vt, \quad y = x_2, \quad z = x_3, \tag{2}$$

the boundary conditions become independent of t and the variables (x_1, t) enter the problem only in the combination $(x_1 - Vt)$. Furthermore, in the new moving Cartesian coordinate system $Oxyz$, partial derivatives w.r.t. t are neglected and (1a) and (1b) can be written as

$$\nabla^2\mathbf{u} + (m^2 - 1)\nabla(\nabla \cdot \mathbf{u}) + \kappa\nabla\theta - m^2c^2\frac{\partial^2\mathbf{u}}{\partial x^2} = 0, \tag{3a}$$

$$\frac{K}{\mu}\nabla^2\theta + C_v\frac{mc}{V_T}\frac{\partial\theta}{\partial x} - \kappa T_0 c V_L\frac{\partial(\nabla \cdot \mathbf{u})}{\partial x} = 0, \tag{3b}$$

where $m = (V_L/V_T) > 1$ with $V_L = [(\lambda + 2\mu)/\rho]^{1/2}$ being the longitudinal (L) wave speed in the *absence* of thermal effects and $V_T = (\mu/\rho)^{1/2}$ being the transverse (T) or shear wave speed, $c \equiv M_L = V/V_L$ and $mc \equiv M_T = V/V_T$ are the two *Mach* numbers, $\kappa = \kappa_0(4 - 3m^2) < 0$, the displacement vector has the components (u_x, u_y, u_z), the stress tensor has the components $(\sigma_{zx}, \sigma_{zy}, \sigma_{zz}, \ldots)$,

$$\nabla \cdot \mathbf{u} = \left(\frac{\partial u_x}{\partial x}\right) + \left(\frac{\partial u_y}{\partial y}\right) + \left(\frac{\partial u_z}{\partial z}\right),$$

and

$$\nabla^2 = \left(\frac{\partial^2}{\partial x^2}\right) + \left(\frac{\partial^2}{\partial y^2}\right) + \left(\frac{\partial^2}{\partial z^2}\right).$$

It is emphasized that V_L above is *not* the longitudinal-wave speed in coupled thermoelasticity but serves in our formulation for a convenient normalization of the field equations.

Finally, the boundary conditions of the problem take the form (see Fig. 1)

$$\sigma_{zz}(x, y, z = 0) = -P\delta(x)\delta(y), \tag{4a}$$

$$\sigma_{zx}(x, y, z = 0) = -S\delta(x)\delta(y), \tag{4b}$$

$$\sigma_{zy}(x, y, z = 0) = 0, \tag{4c}$$

$$\frac{\partial\theta(x, y, z = 0)}{\partial z} = -Q\delta(x)\delta(y), \tag{4d}$$

which hold for $-\infty < x < +\infty$ and $-\infty < y < +\infty$. In the above equations, $\delta(\ )$ is the Dirac delta distribution. The objective of the present work is to determine the displacement field for the problem described by Eqs. (1c), (3) and (4).

3. Basic Radon-transform analysis

The solution of the problem described in Section 2 will be obtained through a technique based on the Radon transform (see e.g. Gel'fand et al., 1966; Ludwig, 1966; Deans, 1983), certain coordinate transformations and elements of distribution theory. This procedure reduces first the original 3D problem to a pair of corresponding *auxiliary* problems, i.e. a 2D plane-strain problem and a 2D anti-plane shear problem. Then, the solution to the original problem follows simply by performing first a coordinate transformation and then taking the inverse Radon transform of the known 2D solutions. Since, in general,

2D problems are easier than their 3D counterparts, solutions to the auxiliary problems can be already available in many cases and this is an advantage of the technique.

The 2D Radon transform of a function $f(\mathbf{r})$, with $|\mathbf{r}| = (x^2 + y^2)^{1/2}$, is defined as

$$\Re(f(\mathbf{r})) \equiv \tilde{f}(q,\omega) = \int\int f(\mathbf{r}) \cdot \delta(q - \mathbf{n}\cdot\mathbf{r})\,\mathrm{d}\mathbf{r} = \int_L f(x,y)\,\mathrm{d}s$$
$$= \int_{-\infty}^{+\infty}\int_{-\infty}^{+\infty} f(x,y)\delta(q - x\cos\omega - y\sin\omega)\,\mathrm{d}x\,\mathrm{d}y, \tag{5}$$

where L denotes *all* straight lines in the plane Oxy (see Fig. 2), and $\mathrm{d}s$ is the infinitesimal length along such a line. The lines L are defined by $\mathbf{n}\cdot\mathbf{r} = q$, with $\mathbf{n} \equiv (n_x, n_y) = (\cos\omega, \sin\omega)$, and the Radon transform is in fact the integral of $f(\mathbf{r})$ over all these straight lines in the plane. The Radon-transform properties of linearity, derivative transformation and transformation of the product of Dirac delta distributions will be used here. These properties are as follows:

$$\Re(C_1 f_1(\mathbf{r}) + C_2 f_2(\mathbf{r})) = C_1\tilde{f}_1(q,\omega) + C_2\tilde{f}_2(q,\omega), \tag{6}$$

$$\Re\left(\frac{\partial f}{\partial x_j}\right) = n_j\frac{\partial\tilde{f}(q,\omega)}{\partial q}, \tag{7}$$

$$\Re\left(\frac{\partial^2 f}{\partial x_j \partial x_k}\right) = n_j n_k\frac{\partial^2\tilde{f}(q,\omega)}{\partial q^2}, \qquad \Re(\nabla^2 f) = \frac{\partial^2\tilde{f}(q,\omega)}{\partial q^2}, \tag{8a, b}$$

$$\Re(\delta(x)\cdot\delta(y)) = \delta(q), \tag{9}$$

where (C_1, C_2) are constants, (j, k) take the values 1 and 2, $(x_1 \equiv x, x_2 \equiv y)$, and ∇^2 now is the 2D Laplace operator (i.e. $\nabla^2 = (\partial^2/\partial x^2) + (\partial^2/\partial y^2)$).

The inverse 2D Radon transform is given by

$$f(x,y) = f(r,\varphi) = -\frac{1}{4\pi^2}\int_0^{2\pi}\left(\int_{-\infty}^{+\infty}\frac{\partial\tilde{f}(q,\omega)}{\partial q}\cdot\mathbf{PF}\left(\frac{1}{q - r\cos(\omega-\varphi)}\right)\mathrm{d}q\right)\mathrm{d}\omega, \tag{10}$$

where the symbol **PF**( ) stands for the *principal-value* pseudo-function (or distribution) (see e.g. Roos, 1969; Kanwal, 1998). In other words, the symbol **PF**( ) means that the inner integral is interpreted in the Cauchy principal-value sense due to a pole of the function ( ). Equivalently, this distribution can be defined as $\langle \mathbf{PF}(1/x), \phi\rangle = \lim_{\tau\to 0}\int_{|x|\geqslant\tau}[\phi(x)/x]\,\mathrm{d}x$, where $\langle,\rangle$ denotes the inner product of distributions, ϕ is a test

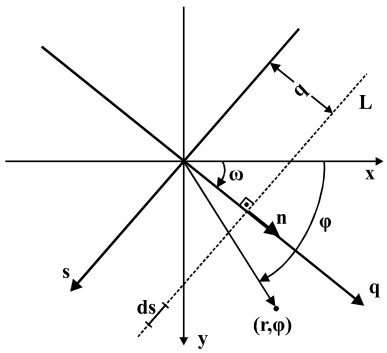

Fig. 2. Geometry for the 2D Radon transform of functions in the xy-plane. The symbol L denotes all straight lines in the plane.

function and τ is a positive number such that $\tau \to 0$. In the analysis below, the case of more than one singularities in the same integrand (i.e. the case of product of distributions) frequently appears and, therefore, the latter notation proves to be convenient.

Next, the two auxiliary problems will be obtained as transformed problems of the original problem. Operating with the Radon transform (5) to Eqs. (3) and (4), and using the properties (6)–(9) provides the following set of transformed field equations and boundary conditions

$$\frac{\partial^2 \tilde{u}_x}{\partial q^2} + \frac{\partial^2 \tilde{u}_x}{\partial z^2} + (m^2 - 1) n_x \frac{\partial}{\partial q}\left(n_x \frac{\partial \tilde{u}_x}{\partial q} + n_y \frac{\partial \tilde{u}_y}{\partial q} + \frac{\partial \tilde{u}_z}{\partial z} \right) + \kappa n_x \frac{\partial \tilde{\theta}}{\partial q} - m^2 c_x^2 \frac{\partial^2 \tilde{u}_x}{\partial q^2} = 0, \tag{11a}$$

$$\frac{\partial^2 \tilde{u}_y}{\partial q^2} + \frac{\partial^2 \tilde{u}_y}{\partial z^2} + (m^2 - 1) n_y \frac{\partial}{\partial q}\left(n_x \frac{\partial \tilde{u}_x}{\partial q} + n_y \frac{\partial \tilde{u}_y}{\partial q} + \frac{\partial \tilde{u}_z}{\partial z} \right) + \kappa n_y \frac{\partial \tilde{\theta}}{\partial q} - m^2 c_x^2 \frac{\partial^2 \tilde{u}_x}{\partial q^2} = 0, \tag{11b}$$

$$\frac{\partial^2 \tilde{u}_z}{\partial q^2} + \frac{\partial^2 \tilde{u}_z}{\partial z^2} + (m^2 - 1) \frac{\partial}{\partial z}\left(n_x \frac{\partial \tilde{u}_x}{\partial q} + n_y \frac{\partial \tilde{u}_y}{\partial q} + \frac{\partial \tilde{u}_z}{\partial z} \right) + \kappa \frac{\partial \tilde{\theta}}{\partial z} - m^2 c_x^2 \frac{\partial^2 \tilde{u}_z}{\partial q^2} = 0, \tag{11c}$$

$$\frac{K}{\mu}\left(\frac{\partial^2 \tilde{\theta}}{\partial q^2} + \frac{\partial^2 \tilde{\theta}}{\partial z^2} \right) + C_v \frac{m c_x}{V_T} \frac{\partial \tilde{\theta}}{\partial q} - \kappa T_0 c_x V_L \frac{\partial}{\partial q}\left(n_x \frac{\partial \tilde{u}_x}{\partial q} + n_y \frac{\partial \tilde{u}_y}{\partial q} + \frac{\partial \tilde{u}_z}{\partial z} \right) = 0, \tag{11d}$$

$$\tilde{\sigma}_{zz}(q, \omega, z = 0) = -P\delta(q), \tag{12a}$$

$$\tilde{\sigma}_{zx}(q, \omega, z = 0) = -S\delta(q), \tag{12b}$$

$$\tilde{\sigma}_{zy}(q, \omega, z = 0) = 0, \tag{12c}$$

$$\frac{\partial \tilde{\theta}(q, \omega, z = 0)}{\partial z} = -Q\delta(q), \tag{12d}$$

where $c_x = c n_x$. Now, as Fig. 3 depicts, we perform a rotation of the original (x, y, z) coordinate system through an angle ω about the z-axis. In the new (q, s, z) coordinate system, Eqs. (11)–(12) are expressed as

$$\frac{\partial^2 \tilde{u}_q}{\partial q^2} + \frac{\partial^2 \tilde{u}_q}{\partial z^2} + (m^2 - 1) \frac{\partial}{\partial q}\left(\frac{\partial \tilde{u}_q}{\partial q} + \frac{\partial \tilde{u}_z}{\partial z} \right) + \kappa \frac{\partial \tilde{\theta}}{\partial q} - m^2 c_x^2 \frac{\partial^2 \tilde{u}_q}{\partial q^2} = 0, \tag{13a}$$

$$\frac{\partial^2 \tilde{u}_z}{\partial q^2} + \frac{\partial^2 \tilde{u}_z}{\partial z^2} + (m^2 - 1) \frac{\partial}{\partial z}\left(\frac{\partial \tilde{u}_q}{\partial q} + \frac{\partial \tilde{u}_z}{\partial z} \right) + \kappa \frac{\partial \tilde{\theta}}{\partial z} - m^2 c_x^2 \frac{\partial^2 \tilde{u}_z}{\partial q^2} = 0, \tag{13b}$$

$$\frac{K}{\mu}\left(\frac{\partial^2 \tilde{\theta}}{\partial q^2} + \frac{\partial^2 \tilde{\theta}}{\partial z^2} \right) + C_v \frac{m c_x}{V_T} \frac{\partial \tilde{\theta}}{\partial q} - \kappa T_0 c_x V_L \frac{\partial}{\partial q}\left(\frac{\partial \tilde{u}_q}{\partial q} + \frac{\partial \tilde{u}_z}{\partial z} \right) = 0, \tag{13c}$$

$$(1 - m^2 c_x^2) \frac{\partial^2 \tilde{u}_s}{\partial q^2} + \frac{\partial^2 \tilde{u}_s}{\partial z^2} = 0, \tag{14}$$

$$\tilde{\sigma}_{zz}(q, \omega, z = 0) = -P\delta(q), \tag{15a}$$

$$\tilde{\sigma}_{zq}(q, \omega, z = 0) = -S\cos\omega\delta(q), \tag{15b}$$

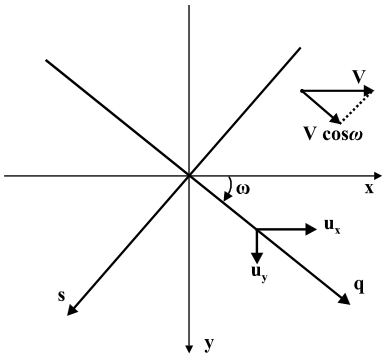

Fig. 3. Initial xy-system and rotated qs-system.

$$\frac{\partial\tilde{\theta}(q,\omega,z=0)}{\partial z}=-Q\delta(q), \tag{15c}$$

$$\tilde{\sigma}_{zs}(q,\omega,z=0)=S\sin\omega\delta(q), \tag{16}$$

where

$$\begin{pmatrix}\tilde{u}_z\\ \tilde{u}_q\\ \tilde{u}_s\end{pmatrix}=\begin{pmatrix}1 & 0 & 0\\ 0 & \cos\omega & \sin\omega\\ 0 & -\sin\omega & \cos\omega\end{pmatrix}\begin{pmatrix}\tilde{u}_z\\ \tilde{u}_x\\ \tilde{u}_y\end{pmatrix}, \tag{17a}$$

$$\begin{pmatrix}\tilde{\sigma}_{zz}\\ \tilde{\sigma}_{zq}\\ \tilde{\sigma}_{zs}\end{pmatrix}=\begin{pmatrix}1 & 0 & 0\\ 0 & \cos\omega & \sin\omega\\ 0 & -\sin\omega & \cos\omega\end{pmatrix}\begin{pmatrix}\tilde{\sigma}_{zz}\\ \tilde{\sigma}_{zx}\\ \tilde{\sigma}_{zy}\end{pmatrix}. \tag{17b}$$

Finally, as expected by the linearity of the operations involved, one may corroborate that the *rotated* Radon-transformed stresses and displacement gradients are related in exactly the same manner as in the physical (non-transformed) plane of the 2D plane-strain and anti-plane shear states. Indeed, it can be shown, by virtue of (1c), (7) and (17), that the following relations hold

$$\tilde{\sigma}_{zz}=(\lambda+2\mu)\frac{\partial\tilde{u}_z}{\partial z}+\lambda\frac{\partial\tilde{u}_q}{\partial q}+\mu\kappa\tilde{\theta}, \tag{18a}$$

$$\tilde{\sigma}_{zq}=\mu\left(\frac{\partial\tilde{u}_z}{\partial q}+\frac{\partial\tilde{u}_q}{\partial z}\right), \tag{18b}$$

$$\tilde{\sigma}_{zs}=\mu\frac{\partial\tilde{u}_s}{\partial z}, \tag{19}$$

which certainly obey the transformed Duhamel–Neumann law $\tilde{\boldsymbol{\sigma}}=\mu(\nabla\tilde{\mathbf{u}}+\tilde{\mathbf{u}}\nabla)+\lambda(\nabla\cdot\tilde{\mathbf{u}})\mathbf{1}+\mu\kappa\tilde{\theta}$, where $\tilde{\mathbf{u}}$ and $\tilde{\boldsymbol{\sigma}}$ have the components $(\tilde{u}_z,\tilde{u}_q,\tilde{u}_s)$ and $(\tilde{\sigma}_{zz},\tilde{\sigma}_{zq},\tilde{\sigma}_{zs},\ldots)$, respectively.

Now, one may observe that Eqs. (13), (15) and (18) form a 2D plane-strain problem in the (q,z) coordinate system. As Fig. 4a depicts, this problem (the *first* auxiliary problem) involves a linearly elastic and thermally conducting body in the form of the half plane $z\geqslant 0$ that is disturbed by the steady-state motion of a concentrated line mechanical/thermal loading. The mechanical load has components P and $S\cos\omega$, whereas the heat source has intensity KQ. The concentrated loads move along the q-axis with velocity

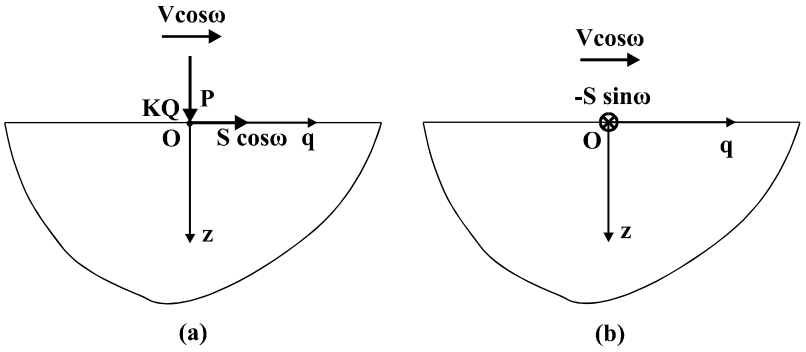

Fig. 4. First (a) and second (b) auxiliary problems in the qz-plane.

$V_q \equiv V\cos\omega$. On the other hand, Eqs. (14), (16) and (19) form a 2D anti-plane shear problem in the (s,z) coordinate system. As Fig. 4b now depicts, this problem (the *second* auxiliary problem) involves a linearly elastic body in the form of the half plane $z \geqslant 0$ that is disturbed by the steady-state motion of a concentrated anti-plane line load. In this case, the problem is 'pure mechanical' and the only load $S\sin\omega$ moves along the q-axis again with velocity $V_q \equiv V\cos\omega$.

4. Results for the first auxiliary problem

In this section, the solution of the first auxiliary problem (2D plane-strain thermo-elastodynamic problem) is recorded. This solution was obtained by Brock and Georgiadis (1997) through two-sided Laplace transforms and exact inversions. Functions in the physical plane of the auxiliary problem are, of course, transformed functions in the Radon-transform plane of the original 3D problem. In using these results, one should be careful in properly interpreting the 2D solution in the *rotated* coordinate system so as the physics of the solution in the new system to be retained. More details on this are given in the end of the present section.

By invoking superposition, the total *normal* displacement at the surface, in the entire speed range, is written as

$$\tilde{u}_z(q,\omega,z=0) = \tilde{u}_z^{(P)}(q,\omega,z=0) + \tilde{u}_z^{(S)}(q,\omega,z=0) + \tilde{u}_z^{(Q)}(q,\omega,z=0), \tag{20}$$

where $(\tilde{u}_z^{(P)}, \tilde{u}_z^{(S)}, \tilde{u}_z^{(Q)})$ are, respectively, the normal displacement due to a normal load P, tangential load $S\cos\omega$ and thermal load KQ. The individual terms at the surface are given by the expressions

$$\tilde{u}_z^{(P)}(q,\omega,z=0) = \frac{P}{\mu}\left[F_1^{(P)}(M_T\cos\omega,\varepsilon)\ln(|q|) - \frac{F_2^{(P)}(M_T\cos\omega,\varepsilon)}{2}\operatorname{sgn}(\operatorname{sgn}(\cos\omega)q)\right], \tag{21}$$

$$\tilde{u}_z^{(S)}(q,\omega,z=0) = \frac{S\cos\omega\operatorname{sgn}(\cos\omega)}{\mu}\left[F_1^{(S)}(M_T\cos\omega,\varepsilon)\ln(|q|) - \frac{F_2^{(S)}(M_T\cos\omega,\varepsilon)}{2}\operatorname{sgn}(\operatorname{sgn}(\cos\omega)q)\right], \tag{22}$$

$$\tilde{u}_z^{(Q)}(q,\omega,z=0) = \frac{Q\kappa h\operatorname{sgn}(\cos\omega)}{(1+\varepsilon)^{1/2}}\left[F_1^{(Q)}(M_T\cos\omega,\varepsilon)\ln|q| - \frac{F_2^{(Q)}(M_T\cos\omega,\varepsilon)}{2}\operatorname{sgn}(\operatorname{sgn}(\cos\omega)q)\right], \tag{23}$$

where sgn( ) is the signum function, $\varepsilon = (T_0/C_v)(\kappa V_T/m)^2$ is the dimensionless coupling constant, $h = KV_T/\mu m C_v$ is the thermoelastic characteristic length, and

$$F_1^{(P)}(M_T,\varepsilon) = \begin{cases} \dfrac{M_T^2(1-M_{L\varepsilon}^2)^{1/2}}{\pi R_\varepsilon} \equiv F_{11}^{(P)}(M_T,\varepsilon), & V < V_T \\ \dfrac{M_T^2(2-M_T^2)^2(1-M_{L\varepsilon}^2)^{1/2}}{\pi K_\varepsilon} \equiv F_{12}^{(P)}(M_T,\varepsilon), & V_T < V < V_{L\varepsilon} \\ 0 \equiv F_{13}^{(P)}(M_T,\varepsilon), & V_{L\varepsilon} < V \end{cases}, \tag{24}$$

$$F_2^{(P)}(M_T,\varepsilon) = \begin{cases} 0 \equiv F_{21}^{(P)}(M_T,\varepsilon), & V < V_T \\ \dfrac{4M_T^2(1-M_{L\varepsilon}^2)(M_T^2-1)^{1/2}}{K_\varepsilon} \equiv F_{22}^{(P)}(M_T,\varepsilon), & V_T < V < V_{L\varepsilon} \\ \dfrac{M_T^2(M_{L\varepsilon}^2-1)^{1/2}}{W_\varepsilon} \equiv F_{23}^{(P)}(M_T,\varepsilon), & V_{L\varepsilon} < V \end{cases}, \tag{25}$$

$$F_1^{(S)}(M_T,\varepsilon) = \begin{cases} 0 \equiv F_{11}^{(S)}(M_T,\varepsilon), & V < V_T \\ -\dfrac{2M_T^2(2-M_T^2)(1-M_{L\varepsilon}^2)^{1/2}(M_T^2-1)^{1/2}}{\pi K_\varepsilon} \equiv F_{12}^{(S)}(M_T,\varepsilon), & V_T < V < V_{L\varepsilon} \\ 0 \equiv F_{13}^{(S)}(M_T,\varepsilon), & V_{L\varepsilon} < V \end{cases}, \tag{26}$$

$$F_2^{(S)}(M_T,\varepsilon) = \begin{cases} \dfrac{(2-M_T^2)-2(1-M_{L\varepsilon}^2)^{1/2}(1-M_T^2)^{1/2}}{R_\varepsilon} \equiv F_{21}^{(S)}(M_T,\varepsilon), & V < V_T \\ \dfrac{(2-M_T^2)^3+8(1-M_{L\varepsilon}^2)(M_T^2-1)}{K_\varepsilon} \equiv F_{22}^{(S)}(M_T,\varepsilon), & V_T < V < V_{L\varepsilon} \\ \dfrac{(2-M_T^2)+2(M_{L\varepsilon}^2-1)^{1/2}(M_T^2-1)^{1/2}}{W_\varepsilon} \equiv F_{23}^{(S)}(M_T,\varepsilon), & V_{L\varepsilon} < V \end{cases}, \tag{27}$$

$$F_1^{(Q)}(M_T,\varepsilon) = \begin{cases} 0 \equiv F_{11}^{(Q)}(M_T,\varepsilon), & V < V_T \\ -\dfrac{4M_{L\varepsilon}(2-M_T^2)(1-M_{L\varepsilon}^2)^{1/2}(M_T^2-1)^{1/2}}{\pi K_\varepsilon} \equiv F_{12}^{(Q)}(M_T,\varepsilon), & V_T < V < V_{L\varepsilon} \\ 0 \equiv F_{13}^{(Q)}(M_T,\varepsilon), & V_{L\varepsilon} < V \end{cases}, \tag{28}$$

$$F_2^{(Q)}(M_T,\varepsilon) = \begin{cases} \dfrac{(2-M_T^2)M_{L\varepsilon}}{R_\varepsilon} \equiv F_{21}^{(Q)}(M_T,\varepsilon), & V < V_T \\ \dfrac{(2-M_T^2)^3 M_{L\varepsilon}}{K_\varepsilon} \equiv F_{22}^{(Q)}(M_T,\varepsilon), & V_T < V < V_{L\varepsilon} \\ \dfrac{(2-M_T^2)M_{L\varepsilon}}{W_\varepsilon} \equiv F_{23}^{(Q)}(M_T,\varepsilon), & V_{L\varepsilon} < V \end{cases}. \tag{29}$$

The above functions depend upon the 'shear' (or 'transverse') Mach number M_T and the coupling constant ε. The orders of magnitude of the coupling constant and the thermoelastic length for usual conducting materials (e.g. aluminum, copper, lead, titanium and steel) are $\varepsilon = O(10^{-2})$ and $h = O(10^{-10})$m. In Eqs. (24)–(29), the following definitions are employed. First, it is noticed that the quantity $V_{L\varepsilon} = V_L(1+\varepsilon)^{1/2}$ represents the *steady-state* velocity of thermoelastic longitudinal waves (Chadwick, 1960; Brock and Georgiadis, 1997)

and, accordingly, the 'thermoelastic longitudinal' Mach number $M_{L\varepsilon} \equiv V/V_{L\varepsilon} = M_L/(1+\varepsilon)^{1/2}$ is defined. Then, the *steady-state* thermoelastic Rayleigh function (Brock and Georgiadis, 1997)

$$R_\varepsilon \equiv R_\varepsilon(M_T, \varepsilon) = (2 - M_T^2)^2 - 4(1 - M_{L\varepsilon}^2)^{1/2}(1 - M_T^2)^{1/2}, \tag{30}$$

defines the steady-state thermoelastic Rayleigh-wave speed $V_{R\varepsilon}$ as the non-trivial *real* root of the equation $R_\varepsilon = 0$, and

$$W_\varepsilon \equiv W_\varepsilon(M_T, \varepsilon) = (2 - M_T^2)^2 + 4(M_{L\varepsilon}^2 - 1)^{1/2}(M_T^2 - 1)^{1/2}, \tag{31}$$

$$K_\varepsilon \equiv K_\varepsilon(M_T, \varepsilon) = (2 - M_T^2)^4 - 16(1 - M_{L\varepsilon}^2)(1 - M_T^2), \tag{32}$$

are functions that are related to the Rayleigh function. In particular, K_ε results as a product by the multiplication of complex conjugates involving the Rayleigh function, at a certain step of the solution procedure of the plane-strain problem. Appendix A of the present work provides a brief analysis concerning the zeroes of K_ε. One of those zeroes coincides with the non-trivial zero of the Rayleigh function R_ε defining therefore the thermoelastic Rayleigh-wave velocity. We should mention that the results of Appendix A were obtained in the spirit of the analysis by Rahman and Barber (1995) on the 'pure elastic' steady-state Rayleigh function.

It is also noticed that the Mach numbers $M_{L\varepsilon}$ and M_T are related, by their definition, through the following equation

$$M_{L\varepsilon} = \frac{1}{m_\varepsilon} M_T, \tag{33}$$

with

$$m_\varepsilon \equiv \frac{V_{L\varepsilon}}{V_T} = \left(\frac{2(1-\nu)(1+\varepsilon)}{(1-2\nu)}\right)^{1/2} > 1, \tag{34}$$

where ν is the Poisson ratio of the material. The last expression may take the form $m_\varepsilon = [2(1-\nu_\varepsilon)/(1-2\nu_\varepsilon)]^{1/2}$ if the new material constant ν_ε is introduced as

$$\nu_\varepsilon = \frac{\nu + \varepsilon(1-\nu)}{1 + 2\varepsilon(1-\nu)}. \tag{35}$$

Further, it can be shown that $\varepsilon/(1+2\varepsilon) \leqslant \nu_\varepsilon \leqslant 1/2$. Finally, we notice that ε is also used as a subscript to emphatically denote that a certain quantity or function depends on thermal effects through the coupling constant.

In the same manner now, one may write by superposition the total *tangential* displacement at the surface. In this case, however, we consider only the subsonic problem ($V < V_T$), in order to avoid the presentation of complicated results, and write

$$\tilde{\boldsymbol{u}}_q(q, \omega, z=0) = \tilde{\boldsymbol{u}}_q^{(P)}(q, \omega, z=0) + \tilde{\boldsymbol{u}}_q^{(S)}(q, \omega, z=0) + \tilde{\boldsymbol{u}}_q^{(Q)}(q, \omega, z=0), \tag{36}$$

where $(\tilde{\boldsymbol{u}}_q^{(P)}, \tilde{\boldsymbol{u}}_q^{(S)}, \tilde{\boldsymbol{u}}_q^{(Q)})$ are the individual tangential displacements due to a normal load P, tangential load $S\cos\omega$ and thermal load KQ, respectively. These displacements are given at the surface by the expressions

$$\tilde{\boldsymbol{u}}_q^{(P)}(q, \omega, z=0) = -\frac{P\,\mathrm{sgn}(\cos\omega)}{2\mu} G^{(P)}(M_T\cos\omega, \varepsilon)\,\mathrm{sgn}(\mathrm{sgn}(\cos\omega)q), \tag{37}$$

$$\tilde{\boldsymbol{u}}_q^{(S)}(q, \omega, z=0) = \frac{S\cos\omega}{\mu} G^{(S)}(M_T\cos\omega, \varepsilon)\ln(|q|), \tag{38}$$

$$\tilde{u}_q^{(Q)}(q,\omega,z=0)=\frac{Q\kappa h}{(1+\varepsilon)^{1/2}}G^{(Q)}(M_{\mathrm{T}}\cos\omega,\varepsilon)\ln(|q|), \tag{39}$$

where the functions of $(M_{\mathrm{T}},\varepsilon)$ that enter the solution are defined as follows:

$$G^{(P)}(M_{\mathrm{T}},\varepsilon)=-\frac{(2-M_{\mathrm{T}}^2)-2(1-M_{\mathrm{L}\varepsilon}^2)^{1/2}(1-M_{\mathrm{T}}^2)^{1/2}}{R_\varepsilon},\quad V<V_{\mathrm{T}}, \tag{40}$$

$$G^{(S)}(M_{\mathrm{T}},\varepsilon)=\frac{M_{\mathrm{T}}^2(1-M_{\mathrm{T}}^2)^{1/2}}{\pi R_\varepsilon},\quad V<V_{\mathrm{T}}, \tag{41}$$

$$G^{(Q)}(M_{\mathrm{T}},\varepsilon)=-\frac{2M_{\mathrm{L}\varepsilon}(1-M_{\mathrm{T}}^2)^{1/2}}{\pi R_\varepsilon},\quad V<V_{\mathrm{T}}. \tag{42}$$

Finally, the total *temperature change* due to mechanical loads is written by superposition as

$$\tilde{\theta}(q,\omega,z=0)=\tilde{\theta}^{(P)}(q,\omega,z=0)+\tilde{\theta}^{(S)}(q,\omega,z=0), \tag{43}$$

where $(\tilde{\theta}^{(P)},\tilde{\theta}^{(S)})$ are the change in temperature due to, respectively, a normal load P and a tangential load $S\cos\omega$. These terms at the surface and for the *entire* velocity range have the following form

$$\tilde{\theta}^{(P)}(q,\omega,z=0)=\frac{P\varepsilon}{\mu\kappa(1+\varepsilon)}\left[L_1^{(P)}(M_{\mathrm{T}}\cos\omega,\varepsilon)\mathbf{PF}\left(\frac{1}{q\,\mathrm{sgn}(\cos\omega)}\right)+L_2^{(P)}(M_{\mathrm{T}}\cos\omega,\varepsilon)\delta(q)\right], \tag{44}$$

$$\tilde{\theta}^{(S)}(q,\omega,z=0)=\frac{S\cos\omega\,\mathrm{sgn}(\cos\omega)\varepsilon}{\mu\kappa(1+\varepsilon)}\left[L_1^{(S)}(M_{\mathrm{T}}\cos\omega,\varepsilon)\mathbf{PF}\left(\frac{1}{q\,\mathrm{sgn}(\cos\omega)}\right)+L_2^{(S)}(M_{\mathrm{T}}\cos\omega,\varepsilon)\delta(q)\right], \tag{45}$$

where the functions of $(M_{\mathrm{T}},\varepsilon)$ now are expressed as follows:

$$L_1^{(P)}(M_{\mathrm{T}},\varepsilon)=\begin{cases}0\equiv L_{11}^{(P)}(M_{\mathrm{T}},\varepsilon), & V<V_{\mathrm{T}}\\ -\dfrac{4M_{\mathrm{T}}^2(2-M_{\mathrm{T}}^2)(1-M_{\mathrm{L}\varepsilon}^2)^{1/2}(M_{\mathrm{T}}^2-1)^{1/2}}{\pi K_\varepsilon}\equiv L_{12}^{(P)}(M_{\mathrm{T}},\varepsilon), & V_{\mathrm{T}}<V<V_{\mathrm{L}\varepsilon},\\ 0\equiv L_{13}^{(P)}(M_{\mathrm{T}},\varepsilon), & V_{\mathrm{L}\varepsilon}<V\end{cases} \tag{46}$$

$$L_2^{(P)}(M_{\mathrm{T}},\varepsilon)=\begin{cases}\dfrac{M_{\mathrm{T}}^2(2-M_{\mathrm{T}}^2)}{R_\varepsilon}\equiv L_{21}^{(P)}(M_{\mathrm{T}},\varepsilon), & V<V_{\mathrm{T}}\\ \dfrac{M_{\mathrm{T}}^2(2-M_{\mathrm{T}}^2)^3}{K_\varepsilon}\equiv L_{22}^{(P)}(M_{\mathrm{T}},\varepsilon), & V_{\mathrm{T}}<V<V_{\mathrm{L}\varepsilon},\\ \dfrac{M_{\mathrm{T}}^2(2-M_{\mathrm{T}}^2)}{W_\varepsilon}\equiv L_{23}^{(P)}(M_{\mathrm{T}},\varepsilon), & V_{\mathrm{L}\varepsilon}<V\end{cases} \tag{47}$$

$$L_1^{(S)}(M_{\mathrm{T}},\varepsilon)=\begin{cases}-\dfrac{2M_{\mathrm{T}}^2(1-M_{\mathrm{T}}^2)^{1/2}}{\pi R_\varepsilon}\equiv L_{11}^{(S)}(M_{\mathrm{T}},\varepsilon), & V<V_{\mathrm{T}}\\ \dfrac{8M_{\mathrm{T}}^2(M_{\mathrm{T}}^2-1)(1-M_{\mathrm{L}\varepsilon}^2)^{1/2}}{\pi K_\varepsilon}\equiv L_{12}^{(S)}(M_{\mathrm{T}},\varepsilon), & V_{\mathrm{T}}<V<V_{\mathrm{L}\varepsilon},\\ 0\equiv L_{13}^{(S)}(M_{\mathrm{T}},\varepsilon), & V_{\mathrm{L}\varepsilon}<V\end{cases} \tag{48}$$

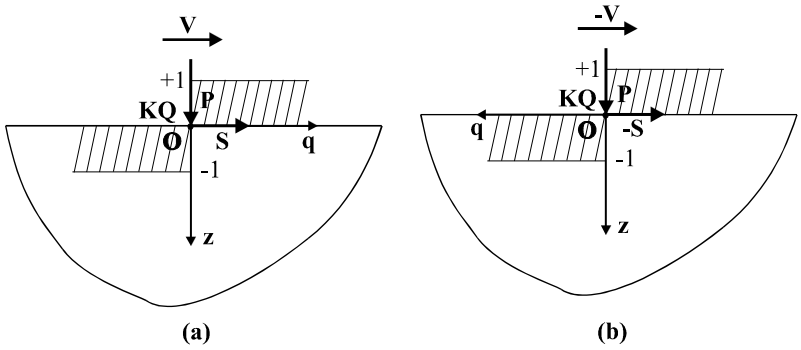

Fig. 5. Schematics for the first auxiliary problem and behavior of the function $\mathrm{sgn}(\mathrm{sgn}(\cos\omega)q)$ in the cases $\omega = 0$ (a) and $\omega = \pi$ (b).

$$L_2^{(S)}(M_T,\varepsilon) = \begin{cases} 0 \equiv L_{21}^{(S)}(M_T,\varepsilon), & V < V_T \\ -\dfrac{2M_T^2(2-M_T^2)^2(M_T^2-1)^{1/2}}{K_\varepsilon} \equiv L_{22}^{(S)}(M_T,\varepsilon), & V_T < V < V_{L\varepsilon} \\ -\dfrac{2M_T^2(M_T^2-1)^{1/2}}{W_\varepsilon} \equiv L_{23}^{(S)}(M_T,\varepsilon), & V_{L\varepsilon} < V \end{cases}. \tag{49}$$

This concludes the presentation of the results for the first auxiliary problem. As mentioned at the beginning of this section, we shall provide now an explanation of the way the results of the 'physical' plane-strain problem in the form obtained by Brock and Georgiadis (1997) have been transferred here and recorded in the form given above. First, consider the function $\mathrm{sgn}(x)$ appearing in particular terms of the solution to the 'physical' problem. In order to preserve this behavior in the auxiliary problem, we should have a Radon transformed solution containing the function $\mathrm{sgn}(q)$ when $\omega \in [0,\pi/2) \cup (3\pi/2, 2\pi]$ (this is because the projection, $V_q = V\cos\omega$, of the velocity V on the q-axis has a positive direction) and the function $\mathrm{sgn}(-q)$ when $\omega \in (\pi/2, 3\pi/2)$ (because now the projection has a negative direction). In a compact form, the Radon transformed solution (i.e. the solution to the first auxiliary problem) that corresponds to the behavior $\mathrm{sgn}(x)$ in the 'physical' plane-strain solution is written as $\mathrm{sgn}(\mathrm{sgn}(\cos\omega)q)$. Accordingly, Fig. 5a and b depicts the first auxiliary problem and the behavior of the function $\mathrm{sgn}(\mathrm{sgn}(\cos\omega)q)$ for the special cases $\omega = 0$ and $\omega = \pi$, respectively. Next, by the same token, one may find that the function $1/x$ appearing in the solution to the 'physical' problem corresponds to the function $1/(\mathrm{sgn}(\cos\omega)q))$ in the solution to the transformed problem. On the contrary, the other functions $\ln|q|$ and $\delta(q)$ do not pose any difficulty because they are even. Finally, one should take into account the *possible* influence of the rotation of the coordinate system upon the direction of the displacements. For instance, the load S in the solution $u_z^{(S)}$ of the 'physical' problem should be taken as the expression $S\cos\omega\,\mathrm{sgn}(\cos\omega)$ when the auxiliary problem is considered and not as the projection $S_q \equiv S\cos\omega$.

5. Solution of the second auxiliary problem

The solution to the second auxiliary problem, i.e. the surface displacement in the elastic half plane $z \geqslant 0$ due to a moving anti-plane shear load, is given by Georgiadis and Lykotrafitis (2001). This solution was obtained by the use of two-sided Laplace transforms and exact inversions. In the anti-plane shear case, only two speed ranges exist (i.e. the subsonic range $|V\cos\omega| < V_T$ and the supersonic $|V\cos\omega| > V_T$ range of the load motion w.r.t. the velocity V_T). In the entire regime, the solution is given in a compact form as

$$\tilde{u}_s^{(S)}(q,\omega,z=0)=\frac{S\sin\omega}{\mu}[Q_1(M_T\cos\omega)\ln(|q|)+Q_2(M_T\cos\omega)H(-\mathrm{sgn}(\cos\omega)q)], \tag{50}$$

where $H(\ )$ is the Heaviside step function, and

$$Q_1(M_T)=\begin{cases}\dfrac{1}{\pi(1-M_T^2)^{1/2}}\equiv Q_{11}(M_T), & V<V_T\\ 0\equiv Q_{12}(M_T), & V>V_T\end{cases}, \tag{51}$$

$$Q_2(M_T)=\begin{cases}0\equiv Q_{21}(M_T), & V<V_T\\ -\dfrac{1}{(M_T^2-1)^{1/2}}\equiv Q_{22}(M_T), & V>V_T\end{cases}. \tag{52}$$

Notice in (50) and for the supersonic case that the argument q of the step function is multiplied by $\mathrm{sgn}(\cos\omega)$ in order for the surface disturbances to be always *behind* the source and not ahead, as the velocity component V_q changes sign in the course of the Radon-transform inversion. Moreover, in utilizing the physical solution in the transformed plane, one should take into account that the direction of the displacement $\tilde{u}_s$ does not depend upon the direction of the motion of the load but does depend upon the direction of the projection of the shear load $S_s\equiv -S\sin\omega$.

It is noticed finally that in the case of a vanishing tangential loading in the original 3D problem, i.e. when ($P\neq 0,\ S=0,\ Q\neq 0$), the solution to the second auxiliary problem is $\tilde{u}_s(q,\omega,z=0)\equiv 0$ since $\tilde{\sigma}_{zs}(q,\omega,z=0)=0$ is obviously the proper boundary condition.

6. Inversion procedure and results for the actual problem

Obtaining the 3D solution from the transformed solution given before is accomplished in two steps. First, the inversion of the coordinate transformation in (17) is performed providing the set $(\tilde{u}_z,\tilde{u}_x,\tilde{u}_y)$ in terms of the rotated Radon-transformed displacements $(\tilde{u}_z,\tilde{u}_q,\tilde{u}_s)$, i.e.

$$\begin{pmatrix}\tilde{u}_z\\ \tilde{u}_x\\ \tilde{u}_y\end{pmatrix}=\begin{pmatrix}1 & 0 & 0\\ 0 & \cos\omega & -\sin\omega\\ 0 & \sin\omega & \cos\omega\end{pmatrix}\begin{pmatrix}\tilde{u}_z\\ \tilde{u}_q\\ \tilde{u}_s\end{pmatrix}. \tag{53}$$

Then, the Radon-transform inversion according to (10) gives the set (u_z,u_x,u_y) in the physical domain. Finally, from the latter solution, one can calculate the displacements in a system of cylindrical polar coordinates (r,φ,z) by using the coordinate transformation (see Fig. 6)

$$\begin{pmatrix}u_z\\ u_r\\ u_\varphi\end{pmatrix}=\begin{pmatrix}1 & 0 & 0\\ 0 & \cos\varphi & \sin\varphi\\ 0 & -\sin\varphi & \cos\varphi\end{pmatrix}\begin{pmatrix}u_z\\ u_x\\ u_y\end{pmatrix} \tag{54}$$

and also evaluate the stresses through (1c).

By using superposition and in order to avoid the presentation of lengthy results and expressions, the displacements due to the loads (P,S,Q) will be considered separately. Also, numerical results will be presented in Section 9.

6.1. Normal displacement $u_z^{(P)}$ due to the normal load P

In this case, the rotation of the original coordinate system (x,y,z) does not affect the transformed component $\tilde{u}_z$, as is seen from (17a), and therefore the second auxiliary problem does not enter the solution

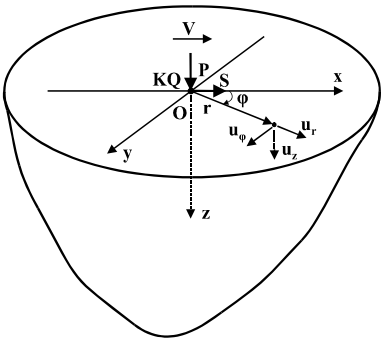

Fig. 6. System of cylindrical polar coordinates (r, φ, z) and corresponding displacement components.

at all. Accordingly, operating with the inverse Radon transform in Eq. (10) on (21) and using the following relations from the theory of distributions (see e.g. Roos, 1969; Kanwal, 1998)

$$\frac{\partial \mathrm{sgn}(\mathrm{sgn}(\cos\omega)q)}{\partial q} = 2\mathrm{sgn}(\cos\omega)\delta(q), \tag{55}$$

$$\frac{\partial \ln(|q|)}{\partial q} = \mathbf{PF}\left(\frac{1}{q}\right), \tag{56}$$

one obtains

$$u_z^{(P)}(r,\varphi,z=0) = -\frac{P}{4\pi^2\mu}\left\{\int_0^{2\pi}\left[F_1^{(P)}(M_\mathrm{T}\cos\omega,\varepsilon)\left(\int_{-\infty}^{+\infty}\mathbf{PF}\left(\frac{1}{q}\right)\mathbf{PF}\left(\frac{1}{q-r\cos(\omega-\varphi)}\right)\mathrm{d}q\right)\right]\mathrm{d}\omega\right.$$
$$\left.-\int_0^{2\pi}\left[\mathrm{sgn}(\cos\omega)F_2^{(P)}(M_\mathrm{T}\cos\omega,\varepsilon)\left(\int_{-\infty}^{+\infty}\mathbf{PF}\left(\frac{1}{q-r\cos(\omega-\varphi)}\right)\delta(q)\,\mathrm{d}q\right)\right]\mathrm{d}\omega\right\}. \tag{57}$$

At this point, we emphasize that any *rigid-body* displacement terms, which could be added in the RHS of (21), have been eliminated by differentiation in the course of inverting the Radon transform. Further, the evaluation of the inner integrals in (57) is accomplished by utilizing additional results from the theory of distributions (Lauwerier, 1963) that concern the Hilbert transform of generalized functions, i.e.

$$\int_{-\infty}^{+\infty}\mathbf{PF}\left(\frac{1}{q}\right)\mathbf{PF}\left(\frac{1}{q-r\cos(\omega-\varphi)}\right)\mathrm{d}q = \pi^2\delta(r\cos(\omega-\varphi)), \tag{58}$$

$$\int_{-\infty}^{+\infty}\mathbf{PF}\left(\frac{1}{q-r\cos(\omega-\varphi)}\right)\delta(q)\,\mathrm{d}q = -\mathbf{PF}\left(\frac{1}{r\cos(\omega-\varphi)}\right). \tag{59}$$

Using now the above results in (57) gives

$$u_z^{(P)}(r,\varphi,z=0) = -\frac{P}{4\mu}\left\{\int_0^{2\pi}\left[F_1^{(P)}(M_\mathrm{T}\cos\omega,\varepsilon)\delta(r\cos(\omega-\varphi))\right]\mathrm{d}\omega\right.$$
$$\left.+\int_0^{2\pi}\left[\mathrm{sgn}(\cos\omega)F_2^{(P)}(M_\mathrm{T}\cos\omega,\varepsilon)\mathbf{PF}\left(\frac{1}{\pi^2 r\cos(\omega-\varphi)}\right)\right]\mathrm{d}\omega\right\}. \tag{60}$$

Further, the following two properties of the Dirac delta distribution are employed: (i) the sifting property, and (ii) the property that

$$\delta[g(\zeta)] = \sum_{j=1}^{N} \frac{\delta(\zeta - a_j)}{|g'(a_j)|},$$

where $g(\zeta)$ is a monotonic real function of ζ which vanishes at the points $\zeta = a_j$, with $(j = 1, 2, \ldots, N)$, and $g'(a_j)$ are the derivatives at the points $\zeta = a_j$ (see e.g. Roos, 1969; Kanwal, 1998). Considering these properties leads to the value $(2/r)F_1^{(P)}(M_T \sin\varphi)$ for the first integral in (60). Also, the second integral is transformed through sectionally monotonic changes of variable as $\zeta = \sin\omega$. In view of the above, Eq. (60) takes the form

$$u_z^{(P)}(r, \varphi, z = 0) = -\frac{P}{\mu r}\left\{\frac{1}{2}F_1^{(P)}(M_T \sin\varphi, \varepsilon) + \frac{\cos\varphi}{\pi^2}\left[\int_0^1 F_2^{(P)}(M_T(1-\zeta^2)^{1/2}, \varepsilon)\mathbf{PF}\left(\frac{1}{\cos^2\varphi - \zeta^2}\right)\mathrm{d}\zeta\right]\right\}. \tag{61}$$

The above result is the basic result for the case of a moving normal load. From the expression in (61), particular results will be obtained below for the entire speed range, i.e. for $0 < V < V_{R\varepsilon}$, $V_{R\varepsilon} < V < V_T$, $V_T < V < V_{L\varepsilon}$ and $V_{L\varepsilon} < V$. The particular results depend of course upon the forms of the functions $F_1^{(P)}(\ )$ and $F_2^{(P)}(\ )$ in each speed range. It is noticed finally that (61) shows that the surface normal displacement $u_z^{(P)}$ is symmetric w.r.t. the x-axis of motion, and this concurs with the physics of the problem.

- Sub-Rayleigh range $(0 < V < V_{R\varepsilon})$:

Here, only the first term in the RHS of (61) contributes, since $F_2^{(P)}(M_T(1-\zeta^2)^{1/2}, \varepsilon) = 0$ for all $\zeta \in [0, 1]$. Thus, the final result is

$$u_z^{(P)}(r, \varphi, z = 0) = -\frac{P}{2\mu r}F_{11}^{(P)}(M_T \sin\varphi, \varepsilon), \tag{62}$$

where the function $F_{11}^{(P)}(\ )$ is given in (24). One may observe that (62) implies the symmetry of $u_z^{(P)}$ w.r.t. both axes x and y.

- Super-Rayleigh subsonic range $(V_{R\varepsilon} < V < V_T)$:

The solution is still given by the first term in the RHS of (61). However, as the analysis in Appendix A indicates, the thermoelastic Rayleigh function vanishes (i.e. $R_\varepsilon(M_T \sin\varphi, \varepsilon) = 0$) along the lines defined by $\varphi = \pm\varphi_{R\varepsilon}$ and $\varphi = \pi \pm \varphi_{R\varepsilon}$ on the half-space surface, where $\varphi_{R\varepsilon} = \sin^{-1}(m_{1\varepsilon}^{1/2}/M_T)$ and $0 < \varphi_{R\varepsilon} < \pi/2$ with $m_{1\varepsilon}$ being the non-trivial zero of $R_\varepsilon(M_T, \varepsilon)$ given by (A.2) of Appendix A in terms of the Poisson's ratio and the coupling constant of the material. Therefore, the normal displacement $u_z^{(P)}$ is singular along these lines. This means that solution (61) in its present form predicts *two* Mach-like Rayleigh wave sectors; one ahead of the moving source and the other behind (see Fig. 7 showing the top view of the problem). Nevertheless, as the pertinent radiation condition requires (see e.g. Fung, 1965), only trailing waves of this type should exist. This statement is also supported by the observation of Barber (1996), in dealing with the respective 'pure mechanical' problem, that the steady-state problem should be viewed as the long-time limit of a *transient* problem, in which the point load (that moves with a super-Rayleigh velocity) is suddenly applied to an initially quiescent half space, and therefore, one should expect in such a problem the existence of Rayleigh-wave disturbances behind but not ahead of the load.

In view of the above, we write the *corrected* solution in this speed range by also taking into account the following three points: (i) The final solution should retain an r^{-1} dependence. This was indicated by Willis (1966), in general 3D problem with concentrated loads, who observed that equilibrium demands that the stress field must vary as r^{-2} from the point of application of the force, and therefore, that the displacement field must vary as r^{-1}. (ii) The expression given by the first term of (61) exhibits symmetry both w.r.t. the axes x and y, whereas the final solution should retain symmetry only w.r.t. the x-axis. (iii) The correction

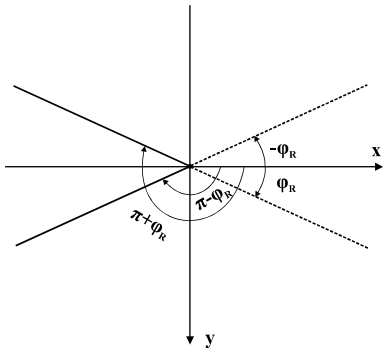

Fig. 7. Mach-like Rayleigh wave 'sectors'. Only the trailing Rayleigh wavefronts (continuous lines) are acceptable in view of the radiation condition.

added should eliminate the thermoelastic Rayleigh-wave disturbance ahead of the load. Therefore, the final solution is written as

$$u_z^{(P)}(r,\varphi,z=0) = -\frac{P}{2\mu}\left[\frac{1}{r}F_{11}^{(P)}(M_T\sin\varphi,\varepsilon) + \frac{\Omega}{r\sin(\varphi-\varphi_{R\varepsilon})} - \frac{\Omega}{r\sin(\varphi+\varphi_{R\varepsilon})}\right], \tag{63}$$

where Ω is a yet unknown constant. Following the relative procedure by Barber (1996), this constant can be determined as follows.

First, we notice from Eqs. (24), (30) and (32) in the main text and Eq. (A.1) in Appendix A that the function $F_{11}^{(P)}(M_T,\varepsilon)$ can be written as

$$F_{11}^{(P)}(M_T,\varepsilon) = \frac{(1-M_{L\varepsilon}^2)^{1/2}[(2-M_T^2)^2 + 4(1-M_{L\varepsilon}^2)^{1/2}(1-M_T^2)^{1/2}]}{\pi(M_T^2-m_{1\varepsilon})(M_T^2-m_{2\varepsilon})(M_T^2-m_{3\varepsilon})}, \tag{64}$$

where $m_{j\varepsilon}$, with ($j=1, 2, 3$), are the non-trivial zeroes of the function K_ε whose expressions are given in Appendix A. Next, the following definitions are introduced

$$A(M_T,\varepsilon) \equiv \frac{4(1-M_{L\varepsilon}^2)}{\prod_{j=1}^{3}(M_T^2-m_{j\varepsilon})}, \qquad B(M_T,\varepsilon) \equiv \frac{(2-M_T^2)^2}{\prod_{j=1}^{3}(M_T^2-m_{j\varepsilon})} \tag{65a,b}$$

and the functions (A, B) are subsequently written as sums of partial fractions through the use of the forms provided in Eqs. (A.5) and (A.6) of Appendix A. In view of the above, $F_{11}^{(P)}(M_T,\varepsilon)$ in (64) takes the following form, which can directly lead to the determination of the constant Ω through canceling of the terms that generate the unacceptable Rayleigh-wave singularities

$$F_{11}^{(P)}(M_T\sin\varphi,\varepsilon) = \frac{1}{\pi}\sum_{j=1}^{3}\frac{A_j(1-M_T^2\sin^2\varphi)^{1/2}}{(M_T^2\sin^2\varphi-m_{j\varepsilon})} + \frac{1}{\pi}\sum_{j=1}^{3}\frac{B_j(1-M_{L\varepsilon}^2\sin^2\varphi)^{1/2}}{(M_T^2\sin^2\varphi-m_{j\varepsilon})}, \tag{66}$$

where the new constants (A_j, B_j), with ($j=1, 2, 3$), are given in Eqs. (A.11) and (A.12) of Appendix A and solely depend upon the Poisson's ratio and the coupling constant of the material. Finally, in view of (66) and the definition of $\varphi_{R\varepsilon}$, (63) becomes

$$u_z^{(P)}(r,\varphi,z=0) = -\frac{P}{2\mu\pi r}\left[\sum_{j=1}^{3}\frac{A_j(1-M_T^2\sin^2\varphi)^{1/2}}{(M_T^2\sin^2\varphi-m_{j\varepsilon})} + \sum_{j=1}^{3}\frac{B_j(1-M_{L\varepsilon}^2\sin^2\varphi)^{1/2}}{(M_T^2\sin^2\varphi-m_{j\varepsilon})} + \frac{2\Omega m_{1\varepsilon}^{1/2}M_T\cos\varphi}{M_T^2\sin^2\varphi-m_{1\varepsilon}}\right]. \tag{67}$$

From the above form, it is clear now that Ω should be chosen so that the terms corresponding to $j = 1$ to be canceled along the Rayleigh wave singularities ahead of the load, that is for $\varphi = \pm\varphi_{R\varepsilon}$. In this way, by solving the equation

$$A_1(1 - M_T^2 \sin^2 \varphi_{R\varepsilon})^{1/2} + B_1(1 - m^{-2}M_T^2 \sin^2 \varphi_{R\varepsilon})^{1/2} + 2\Omega m_1^{1/2} M_T \cos \varphi_{R\varepsilon} = 0, \tag{68}$$

we obtain the appropriate value of Ω as

$$\Omega = -\frac{M_T(1 - m_\varepsilon^{-2}m_{1\varepsilon})^{1/2}[(2 - m_{1\varepsilon})^2 + 4(1 - m_{1\varepsilon})^{1/2}(1 - m_\varepsilon^{-2}m_{1\varepsilon})^{1/2}]}{2m_{1\varepsilon}^{1/2} M_T (M_T^2 - m_{1\varepsilon})^{1/2}(m_{1\varepsilon} - m_{2\varepsilon})(m_{1\varepsilon} - m_{3\varepsilon})}. \tag{69}$$

Further, from (67) the final solution in the range $V_R < V < V_T$ is obtained as

$$u_z^{(P)}(r, \varphi, z = 0) = -\frac{P}{2\mu\pi r}\left[\pi F_{11}^{(P)}(M_T \sin\varphi, \varepsilon) - \frac{M_T \cos\varphi(1 - m_\varepsilon^{-2}m_{1\varepsilon})^{1/2}[(2 - m_{1\varepsilon})^2 + 4(1 - m_{1\varepsilon})^{1/2}(1 - m_\varepsilon^{-2}m_{1\varepsilon})^{1/2}]}{(M_T^2 \sin^2\varphi - m_{1\varepsilon})(M_T^2 - m_{1\varepsilon})^{1/2}(m_{1\varepsilon} - m_{2\varepsilon})(m_{1\varepsilon} - m_{3\varepsilon})}\right]. \tag{70}$$

- Transonic range ($V_T < V < V_{L\varepsilon}$):

In this case, both terms in the RHS of (61) contribute. Also, the functions $F_1^{(P)}(M_T \sin\varphi, \varepsilon)$ and $F_2^{(P)}(M_T \sin\varphi, \varepsilon)$ because of (24), (25), (64), (65a,b) and (A.1) are written as

$$\pi F_1^{(P)}(M_T \sin\varphi, \varepsilon) = A(M_T \sin\varphi, \varepsilon)(1 - M_T^2 \sin^2\varphi)^{1/2} H(V_T - V|\sin\varphi|) + B(M_T \sin\varphi, \varepsilon)(1 - M_{L\varepsilon}^2 \sin^2\varphi)^{1/2}, \tag{71a}$$

$$F_2^{(P)}(M_T(1 - \zeta^2)^{1/2}, \varepsilon) = A(M_T(1 - \zeta^2)^{1/2}, \varepsilon)(M_T^2 - M_T^2\zeta^2 - 1)^{1/2} H(V(1 - \zeta^2)^{1/2} - V_T). \tag{71b}$$

Substituting then (71) in (61) provides

$$u_z^{(P)}(r, \varphi, z = 0) = -\frac{P}{2\mu\pi r}[A(M_T \sin\varphi, \varepsilon)(1 - M_T^2 \sin^2\varphi)^{1/2} H(V_T - V|\sin\varphi|) + B(M_T \sin\varphi, \varepsilon) \times (1 - M_{L\varepsilon}^2 \sin^2\varphi)^{1/2}] - \frac{P\cos\varphi}{\mu\pi^2 r}\int_0^{[1-(1/M_T^2)]^{1/2}} A(M_T(1 - \zeta^2)^{1/2}, \varepsilon)(M_T^2 - M_T^2\zeta^2 - 1)^{1/2} \times \mathbf{PF}\left(\frac{1}{\cos^2\varphi - \zeta^2}\right) d\zeta. \tag{72}$$

An analysis now of the integral in the RHS of (72) is provided and this shows that the integral is a well-defined Cauchy *principal-value* integral. In view of (65a), the following points are noted about the integral: (i) The analysis in Appendix A shows that the zero of the term $M_T^2 - m_{1\varepsilon} - M_T^2\zeta^2$ lies outside the integration interval. (ii) The terms $M_T^2 - m_{j\varepsilon} - M_T^2\zeta^2$, with ($j = 2, 3$), do not have zeroes in this velocity regime because it is valid that $m_{3\varepsilon} > m_{2\varepsilon} > M_T^2$, as shown in Appendix A. (iii) Along those angles φ defined by $\cos^2\varphi = 0$, the integral diverges but because of the concurrent vanishing of the coefficient $\cos\varphi$ the integral term in (72) eventually vanishes. (iv) Along those angles φ defined by $\cos^2\varphi = [1 - (1/M_T^2)]$ (these angles correspond to the shear Mach wavefronts), the integrand exhibits an integrable behavior and varies as $([1 - (1/M_T^2)]^{1/2} - \zeta)^{-1/2}$.

The above analysis reveals therefore that the integrand in (72) exhibits only one pole at $\zeta = |\cos\varphi|$, and the associated integral is a Cauchy *principal-value* integral contributing *no* singularity in the displacement. The only singularity in (72) stems from the first term of this expression and is associated with thermoelastic Rayleigh wavefronts. As in the previous super-Rayleigh/subsonic case, these wavefronts extend both ahead

of the load and behind the load. We can work therefore as before to eliminate the singularity ahead of the moving load. The first term in (72) also indicates the existence of trailing shear Mach wavefronts since it contains the Heaviside step function $H(V_T - V|\sin\varphi|)$. In view of the above, the final expression for the surface normal displacement $u_z^{(P)}$ due to a normal load P moving in the transonic range is found to be

$$u_z^{(P)}(r,\varphi,z=0) = -\frac{P}{2\mu\pi r}\left[A(M_T\sin\varphi,\varepsilon)(1-M_T^2\sin^2\varphi)^{1/2}H(V_T - V|\sin\varphi|) + B(M_T\sin\varphi,\varepsilon)\right.$$
$$\left.\times(1-M_{L\varepsilon}^2\sin^2\varphi)^{1/2} - \frac{M_T\cos\varphi(1-m_\varepsilon^{-2}m_{1\varepsilon})^{1/2}[(2-m_{1\varepsilon})^2+4(1-m_{1\varepsilon})^{1/2}(1-m_\varepsilon^{-2}m_{1\varepsilon})^{1/2}]}{(M_T^2\sin^2\varphi-m_{1\varepsilon})(M_T^2-m_{1\varepsilon})^{1/2}(m_{1\varepsilon}-m_{2\varepsilon})(m_{1\varepsilon}-m_{3\varepsilon})}\right]$$
$$-\frac{P\cos\varphi}{\mu\pi^2 r}\int_0^{[1-(1/M_T^2)]^{1/2}} A(M_T(1-\zeta^2)^{1/2},\varepsilon)(M_T^2-M_T^2\zeta^2-1)^{1/2}\mathbf{PF}\left(\frac{1}{\cos^2\varphi-\zeta^2}\right)d\zeta. \tag{73}$$

The Cauchy *principal-value* integral in (73) and all other integrals obtained below as analytical solutions were evaluated by using the *numerical* algorithms of the program MATHEMATICA™. In all cases analytical considerations are provided to show that these integrals are amenable to a direct numerical treatment. Numerical results are given in Section 9.

- Supersonic range ($V_{L\varepsilon} < V$):

Substituting (24) and (25) in the basic result (61) and taking into account (65) and (A.1), the following expression is obtained

$$u_z^{(P)}(r,\varphi,z=0) = -\frac{P}{2\mu\pi r}[A(M_T\sin\varphi,\varepsilon)(1-M_T^2\sin^2\varphi)^{1/2}H(V_T - V|\sin\varphi|) + B(M_T\sin\varphi,\varepsilon)$$
$$\times(1-M_{L\varepsilon}^2\sin^2\varphi)^{1/2}H(V_{L\varepsilon}-V|\sin\varphi|)] - \frac{P\cos\varphi}{\mu\pi^2 r}\int_0^{[1-(1/M_{L\varepsilon}^2)]^{1/2}}[A(M_T(1-\zeta^2)^{1/2},\varepsilon)$$
$$\times(M_T^2-M_T^2\zeta^2-1)^{1/2} + B(M_T(1-\zeta^2)^{1/2},\varepsilon)(M_{L\varepsilon}^2-M_{L\varepsilon}^2\zeta^2-1)^{1/2}]\mathbf{PF}\left(\frac{1}{\cos^2\varphi-\zeta^2}\right)d\zeta$$
$$-\frac{P\cos\varphi}{\mu\pi^2 r}\int_{[1-(1/M_{L\varepsilon}^2)]^{1/2}}^{[1-(1/M_T^2)]^{1/2}} A(M_T(1-\zeta^2)^{1/2},\varepsilon)(M_T^2-M_T^2\zeta^2-1)^{1/2}\mathbf{PF}\left(\frac{1}{\cos^2\varphi-\zeta^2}\right)d\zeta. \tag{74}$$

In the RHS of (74), the first term with the two Heaviside step functions clearly exhibits the appearance of the longitudinal and shear Mach wavefronts. However, the second and third terms (integral terms) require a more careful analysis.

For the first integral the following points are noticed. (i) Relation (34) and the analysis in Appendix A indicate that $m_{1\varepsilon} < m_\varepsilon^2$ and, therefore, the term $M_T^2 - m_{1\varepsilon} - M_T^2\zeta^2$ has no zeros inside the integration interval. (ii) The analysis in Appendix A indicates that the zeros $m_{2\varepsilon}$ and $m_{3\varepsilon}$ of the function $K_\varepsilon(M_T,\varepsilon)$ are real numbers when the material constant v_ε defined in (35) satisfies the inequalities $0 \leqslant v_\varepsilon \leqslant v_0 \equiv 0.2630820648\ldots$ In addition, in the supersonic regime, the inequalities $m_{2\varepsilon} < M_T^2$ and/or $m_{3\varepsilon} < M_T^2$ may be satisfied and, accordingly, the zeroes of the terms $M_T^2 - m_{j\varepsilon} - M_T^2\zeta^2$, with ($j = 2, 3$), may lie *within* the integration interval. Nevertheless, it can be shown that these points correspond to removable singularities. (iii) Along the lines defined by $\cos^2\varphi = [1-(1/M_{L\varepsilon}^2)]$, which correspond to the longitudinal Mach wavefronts, the integrand remains integrable since it behaves as $([1-(1/M_{L\varepsilon}^2)]^{1/2}-\zeta)^{-1/2}$ at the upper integration limit.

For the second integral now, the following points are of notice. (i) The zeroes of the term $M_T^2 - m_{1\varepsilon} - M_T^2\zeta^2$ lie outside the integration interval, since $m_{1\varepsilon} < 1$. (ii) The zeros of the terms $M_T^2 - m_{j\varepsilon} - M_T^2\zeta^2$, with ($j = 2, 3$), lie outside the integration interval. (iii) Along the shear Mach wavefront (upper integration

limit), the integrand behaves like an inverse square root and is, therefore, integrable. Along the longitudinal Mach wavefront, the integrand is smooth.

Finally, we observe that in the two integrands of (74) only one pole appears at the point $\zeta = |\cos\varphi|$. Therefore, the integrals can be evaluated in the Cauchy *principal-value* sense without any particular difficulty. In view of the above observations, it is concluded that there are no other singularities for the surface normal displacement $u_z^{(P)}(r,\varphi,z=0)$ except for the Rayleigh-type singularity exhibited by the first (non-integral) term of (74). This singularity is due to the functions $A(M_T\sin\varphi,\varepsilon)$ and $B(M_T\sin\varphi,\varepsilon)$. Following the same procedure as in the cases of super-Rayleigh/subsonic and transonic ranges treated before, the final form of the solution in the supersonic range is found to be

$$\begin{aligned}
u_z^{(P)}(r,\varphi,z=0) = -\frac{P}{2\mu\pi r}\Bigg[& A(M_T\sin\varphi,\varepsilon)(1-M_T^2\sin^2\varphi)^{1/2}H(V_T-V|\sin\varphi|) + B(M_T\sin\varphi,\varepsilon) \\
& \times (1-M_{L\varepsilon}^2\sin^2\varphi)^{1/2}H(V_{L\varepsilon}-V|\sin\varphi|) \\
& - \frac{M_T\cos\varphi(1-m_\varepsilon^{-2}m_{1\varepsilon})^{1/2}[(2-m_{1\varepsilon})^2+4(1-m_{1\varepsilon})^{1/2}(1-m_\varepsilon^{-2}m_{1\varepsilon})^{1/2}]}{(M_T^2\sin^2\varphi-m_{1\varepsilon})(M_T^2-m_{1\varepsilon})^{1/2}(m_{1\varepsilon}-m_{2\varepsilon})(m_{1\varepsilon}-m_{3\varepsilon})}\Bigg] \\
& - \frac{P\cos\varphi}{\mu\pi^2 r}\int_0^{[1-(1/M_{L\varepsilon}^2)]^{1/2}} B(M_T(1-\zeta^2)^{1/2},\varepsilon)(M_{L\varepsilon}^2-M_{L\varepsilon}^2\zeta^2-1)^{1/2}\mathbf{PF}\left(\frac{1}{\cos^2\varphi-\zeta^2}\right)\mathrm{d}\zeta \\
& - \frac{P\cos\varphi}{\mu\pi^2 r}\int_0^{[1-(1/M_{L\varepsilon}^2)]^{1/2}} A(M_T(1-\zeta^2)^{1/2},\varepsilon)(M_T^2-M_T^2\zeta^2-1)^{1/2}\mathbf{PF}\left(\frac{1}{\cos^2\varphi-\zeta^2}\right)\mathrm{d}\zeta \\
& - \frac{P\cos\varphi}{\mu\pi^2 r}\int_{[1-(1/M_{L\varepsilon}^2)]^{1/2}}^{[1-(1/M_T^2)]^{1/2}} A(M_T(1-\zeta^2)^{1/2},\varepsilon)(M_T^2-M_T^2\zeta^2-1)^{1/2}\mathbf{PF}\left(\frac{1}{\cos^2\varphi-\zeta^2}\right)\mathrm{d}\zeta.
\end{aligned} \tag{75}$$

With the above expression, the presentation of results for the surface normal displacement $u_z^{(P)}$ is concluded. In the limit as $\varepsilon\to 0$, i.e. as thermal effects are eliminated, these results take the form of the results for the 'pure mechanical' problem of a normal load moving over the surface of an elastic half space (Georgiadis and Lykotrafitis, 2001). Notice also that the results of Georgiadis and Lykotrafitis (2001) agree with the ones of Lansing (1966) and Barber (1996) in the entire speed range, and with the sub-Rayleigh results of Eason (1965), who restricted himself in a sub-Rayleigh analysis of the problem only.

6.2. Vertical displacement $u_z^{(S)}$ due to the tangential load S

We operate again with the inverse Radon transform on (22) and proceed as in the previous case of the normal load obtaining the following basic result

$$\begin{aligned}
u_z^{(S)}(r,\varphi,z=0) = & -\frac{S}{2\mu r}F_1^{(S)}(M_T\sin\varphi,\varepsilon)|\sin\varphi| - \frac{S\cos\varphi}{\mu\pi^2 r} \\
& \times \int_0^1 F_2^{(S)}(M_T(1-\zeta^2)^{1/2},\varepsilon)(1-\zeta^2)^{1/2}\mathbf{PF}\left(\frac{1}{\cos^2\varphi-\zeta^2}\right)\mathrm{d}\zeta.
\end{aligned} \tag{76}$$

From this expression, particular results will be obtained below for the entire speed regime, i.e. for $0<V<V_{R\varepsilon}$, $V_{R\varepsilon}<V<V_T$, $V_T<V<V_{L\varepsilon}$ and $V_{L\varepsilon}<V$. These results will depend of course upon the particular forms of the functions $F_1^{(S)}(\ )$ and $F_2^{(S)}(\ )$ in each speed range. One may observe finally that Eq. (76) clearly exhibits the required symmetry of $u_z^{(S)}$ w.r.t. the x-axis.

- Sub-Rayleigh range ($0 < V < V_{R\varepsilon}$):

In this range, only the integral in (76) contributes, because $F_{11}^{(S)}(M_T \sin\varphi) = 0$ for all angles φ, giving the result

$$u_z^{(S)}(r,\varphi,z=0) = -\frac{S\cos\varphi}{\mu\pi^2 r}\int_0^1 [C(M_T(1-\zeta^2)^{1/2},\varepsilon) + D(M_T(1-\zeta^2)^{1/2},\varepsilon)(1-M_T^2+M_T^2\zeta^2)^{1/2} \times (1-M_{L\varepsilon}^2+M_{L\varepsilon}^2\zeta^2)^{1/2}](1-\zeta^2)^{1/2}\mathbf{PF}\left(\frac{1}{\cos^2\varphi-\zeta^2}\right)\mathrm{d}\zeta, \tag{77}$$

where

$$C(M_T,\varepsilon) = \frac{(8m_\varepsilon^{-2}-4)+(6-8m_\varepsilon^{-2})M_T^2 - M_T^4}{\prod_{j=1}^3 (M_T^2 - m_{j\varepsilon})}, \qquad D(M_T,\varepsilon) = \frac{2(2-M_T^2)}{\prod_{j=1}^3 (M_T^2 - m_{j\varepsilon})}. \tag{78a, b}$$

If we set $\varepsilon = 0$ in (77), the respective results of Eason (1965) and Georgiadis and Lykotrafitis (2001) are recovered.

- Super-Rayleigh subsonic range ($V_{R\varepsilon} < V < V_T$):

In this case, examining (76) reveals that there are two poles at the points $\zeta = [1-(m_{1\varepsilon}/M_T^2)]^{1/2}$ and $\zeta = |\cos\varphi|$. No additional poles arise since the terms $M_T^2 - m_{j\varepsilon} - M_T^2\zeta^2$, with ($j = 2, 3$), exhibit no zeros (see Appendix A). One therefore may obtain

$$u_z^{(S)}(r,\varphi,z=0) = -\frac{S\cos\varphi}{\mu\pi^2 r}\int_0^1 [C^*(M_T(1-\zeta^2)^{1/2},\varepsilon) + D^*(M_T(1-\zeta^2)^{1/2},\varepsilon)(1-M_T^2+M_T^2\zeta^2)^{1/2} \times (1-M_{L\varepsilon}^2+M_{L\varepsilon}^2\zeta^2)^{1/2}](1-\zeta^2)^{1/2}\mathbf{PF}\left(\frac{1}{M_T^2-m_{1\varepsilon}-M_T^2\zeta^2}\right)\mathbf{PF}\left(\frac{1}{\cos^2\varphi-\zeta^2}\right)\mathrm{d}\zeta, \tag{79}$$

where

$$C^*(M_T,\varepsilon) = C(M_T,\varepsilon)(M_T^2 - m_{1\varepsilon}), \qquad D^*(M_T,\varepsilon) = D(M_T,\varepsilon)(M_T^2 - m_{1\varepsilon}). \tag{80a, b}$$

For those angles that the two poles in the integrand of (79) do not coincide, no difficulty arises for the numerical evaluation of the integral. The two poles coincide when $\cos^2\varphi = [1-(m_{1\varepsilon}/M_T^2)]$, which are directions corresponding to the Rayleigh Mach wavefronts. A double pole then arises and the solution takes the form

$$u_z^{(S)}(r,\varphi,z=0) = -\frac{S\cos\varphi}{\mu\pi^2 r}\int_0^1 [C^*(M_T(1-\zeta^2)^{1/2},\varepsilon) + D^*(M_T(1-\zeta^2)^{1/2},\varepsilon)(1-M_T^2+M_T^2\zeta^2)^{1/2} \times (1-M_{L\varepsilon}^2+M_{L\varepsilon}^2\zeta^2)^{1/2}](1-\zeta^2)^{1/2}\frac{1}{M_T^2}\mathbf{PF}\left(\frac{1}{([1-(m_{1\varepsilon}/M_T^2)]-\zeta^2)^2}\right)\mathrm{d}\zeta, \tag{81}$$

where $\mathbf{PF}(\ )$ denotes now the *finite-part* (or *second-order* principal-part) pseudo-function or distribution (see e.g. Roos, 1969; Kanwal, 1998). In other words, the integral in (81) should be interpreted as a Hadamard *finite-part* integral in the sense that

$$\langle \mathbf{PF}(1/x^2), \phi\rangle = \lim_{\tau\to 0}\int_{|x|\geqslant\tau}\frac{\phi(x)-\phi(0)}{x^2}\,\mathrm{d}x.$$

Equivalently, the second-order principal-part pseudo-function is the negative of the derivative of the principal-value pseudo-function, i.e. $\mathbf{PF}(1/x^2) = -\mathbf{PF}'(1/x)$. In view of the above, the displacement $u_z^{(S)}$ given by (81) remains bounded even along the Rayleigh wavefronts.

- Transonic range ($V_T < V < V_{L\varepsilon}$):
  One may work as in the latter case and combine now Eqs. (26), (27), (76), (78) and (80). The result is

$$\begin{aligned} u_z^{(S)}(r,\varphi,z=0) = {} & \frac{S|\sin\varphi|}{2\mu\pi r} D(M_T\sin\varphi,\varepsilon)(1-M_{L\varepsilon}^2\sin^2\varphi)^{1/2}(M_T^2\sin^2\varphi-1)^{1/2} H\left(|\sin\varphi|-\frac{1}{M_T}\right) \\ & -\frac{S\cos\varphi}{\mu\pi^2 r}\left[\int_0^1 C^*(M_T(1-\zeta^2)^{1/2},\varepsilon)(1-\zeta^2)^{1/2}\mathbf{PF}\left(\frac{1}{M_T^2-m_{1\varepsilon}-M_T^2\zeta^2}\right)\right. \\ & \times \mathbf{PF}\left(\frac{1}{\cos^2\varphi-\zeta^2}\right)\mathrm{d}\zeta + \int_{[1-(1/M_T^2)]^{1/2}}^1 D^*(M_T(1-\zeta^2)^{1/2},\varepsilon)(1-M_T^2+M_T^2\zeta^2)^{1/2} \\ & \left.\times (1-M_{L\varepsilon}^2+M_{L\varepsilon}^2\zeta^2)^{1/2}(1-\zeta^2)^{1/2}\mathbf{PF}\left(\frac{1}{M_T^2-m_{1\varepsilon}-M_T^2\zeta^2}\right)\mathbf{PF}\left(\frac{1}{\cos^2\varphi-\zeta^2}\right)\mathrm{d}\zeta\right]. \end{aligned} \tag{82}$$

The first integrand in (82) exhibits poles at the points $\zeta = [1-(m_{1\varepsilon}/M_T^2)]^{1/2}$ and $\zeta = |\cos\varphi|$. The second integrand exhibits always a pole at $\zeta = [1-(m_{1\varepsilon}/M_T^2)]^{1/2}$, and a pole at $\zeta = |\cos\varphi|$ only when $\cos^2\varphi > [1-(1/M_T^2)]$. Both integrals are evaluated as Cauchy *principal-value* integrals.

- Supersonic range ($V_{L\varepsilon} < V$):
  Here, Eqs. (26), (27), (76), (78) and (80) provide

$$\begin{aligned} u_z^{(S)}(r,\varphi,z=0) = {} & \frac{S|\sin\varphi|}{2\mu\pi r} D(M_T\sin\varphi,\varepsilon)(1-M_{L\varepsilon}^2\sin^2\varphi)^{1/2}(M_T^2\sin^2\varphi-1)^{1/2} \\ & \times\left[H\left(|\sin\varphi|-\frac{1}{M_T}\right)-H\left(|\sin\varphi|-\frac{1}{M_{L\varepsilon}}\right)\right] \\ & -\frac{S\cos\varphi}{\mu\pi^2 r}\left[\int_0^1 C(M_T(1-\zeta^2)^{1/2},\varepsilon)(1-\zeta^2)^{1/2}\mathbf{PF}\left(\frac{1}{\cos^2\varphi-\zeta^2}\right)\mathrm{d}\zeta\right. \\ & -\int_0^{[1-(1/M_{L\varepsilon}^2)]^{1/2}} D(M_T(1-\zeta^2)^{1/2},\varepsilon)(M_T^2-M_T^2\zeta^2-1)^{1/2}(M_{L\varepsilon}^2-M_{L\varepsilon}^2\zeta^2-1)^{1/2} \\ & \times(1-\zeta^2)^{1/2}\mathbf{PF}\left(\frac{1}{\cos^2\varphi-\zeta^2}\right)\mathrm{d}\zeta + \int_{[1-(1/M_T^2)]^{1/2}}^1 D(M_T(1-\zeta^2)^{1/2},\varepsilon) \\ & \left.\times(1-M_T^2+M_T^2\zeta^2)^{1/2}(1-M_{L\varepsilon}^2+M_{L\varepsilon}^2\zeta^2)^{1/2}(1-\zeta^2)^{1/2}\mathbf{PF}\left(\frac{1}{\cos^2\varphi-\zeta^2}\right)\mathrm{d}\zeta\right]. \end{aligned} \tag{83}$$

As for the numerical evaluation of (83), one encounters no difficulties except in the case that the material constant v_ε is in the range $0 \leqslant v_\varepsilon \leqslant v_0$. This is because the zeros of the function $K_\varepsilon(M_T,\varepsilon)$ are real and, therefore, the integrands in the integration intervals $[0,1]$ and $[0,(1-1/M_{L\varepsilon}^2)^{1/2}]$ may exhibit more than two distinct poles. Since this case poses a difficulty in the numerical treatment, we should write the terms $C(M_T(1-\zeta^2)^{1/2},\varepsilon)$ and $D(M_T(1-\zeta^2)^{1/2},\varepsilon)$ as partial fractions according to Eqs. (A.7), (A.8), (A.13) and (A.14) of Appendix A. In this way, the first two integrals in (83), say I_1 and I_2, are written in the following forms that are convenient for numerical treatment

$$I_1 = \sum_{j=1}^{3} C_j \int_0^1 \mathbf{PF}\left(\frac{1}{M_T^2 - m_{j\varepsilon} - M_T^2\zeta^2}\right)\mathbf{PF}\left(\frac{1}{\cos^2\varphi - \zeta^2}\right)(1-\zeta^2)^{1/2}\,\mathrm{d}\zeta, \tag{84}$$

$$I_2 = \sum_{j=1}^{3} D_j \int_0^{[1-(1/M_{L\varepsilon}^2)]^{1/2}} \mathbf{PF}\left(\frac{1}{M_T^2 - m_{j\varepsilon} - M_T^2\zeta^2}\right)(M_T^2 - M_T^2\zeta^2 - 1)^{1/2}(M_{L\varepsilon}^2 - M_{L\varepsilon}^2\zeta^2 - 1)^{1/2}(1-\zeta^2)^{1/2} \times \mathbf{PF}\left(\frac{1}{\cos^2\varphi - \zeta^2}\right)\mathrm{d}\zeta, \tag{85}$$

where the constants (C_j, D_j) are given in Eqs. (A.13) and (A.14) of Appendix A. These constants are expressed in terms of the non-trivial zeroes ($m_{1\varepsilon}, m_{2\varepsilon}, m_{3\varepsilon}$) of the function K_ε and depend solely upon the Poisson's ratio and the coupling constant of the material.

6.3. Normal displacement $u_z^{(Q)}$ due to the heat source KQ

Working as in the previous cases and operating with (10) on (23), one may get the following result, which holds for the entire velocity range

$$u_z^{(Q)}(r,\varphi,z=0) = -\frac{Q\kappa h}{2(1+\varepsilon)^{1/2}r}F_1^{(Q)}(M_T\sin\varphi,\varepsilon)\mathrm{sgn}(\sin\varphi) - \frac{Q\kappa h\cos\varphi}{(1+\varepsilon)^{1/2}\pi^2 r}\int_0^1 F_2^{(Q)}(M_T(1-\zeta^2)^{1/2},\varepsilon)\mathbf{PF}\left(\frac{1}{\cos^2\varphi-\zeta^2}\right)\mathrm{d}\zeta. \tag{86}$$

As usual, from this general expression specific results in forms that allow direct numerical evaluation will be obtained in each particular range. One may observe that the form in (86) bears resemblance with the respective form giving $u_z^{(S)}$, so no details for the present case are given below and only the final expressions are recorded.

- Sub-Rayleigh range ($0 < V < V_{R\varepsilon}$):

In this case, only the integral term in (86) contributes to $u_z^{(Q)}$ since $F_1^{(Q)}(M_T\sin\varphi,\varepsilon) = 0$. Then, we multiply both the numerator and denominator of the integrand by the function $(2 - M_T^2 + M_T^2\zeta^2)^2 + 4(1 - M_T^2 + M_T^2\zeta^2)^{1/2}(1 - M_{L\varepsilon}^2 + M_{L\varepsilon}^2\zeta^2)^{1/2}$ and use Eq. (A.1) of Appendix A obtaining the result

$$u_z^{(Q)}(r,\varphi,z=0) = -\frac{Q\kappa h\cos\varphi}{(1+\varepsilon)^{1/2}\pi^2 r}\int_0^1 E(M_T(1-\zeta^2)^{1/2},\varepsilon)M_{L\varepsilon}(1-\zeta^2)^{1/2}\mathbf{PF}\left(\frac{1}{\cos^2\varphi-\zeta^2}\right)\mathrm{d}\zeta - \frac{Q\kappa h\cos\varphi}{(1+\varepsilon)^{1/2}\pi^2 r}\int_0^1 N(M_T(1-\zeta^2)^{1/2},\varepsilon)(1-M_T^2+M_T^2\zeta^2)^{1/2}(1-M_{L\varepsilon}^2+M_{L\varepsilon}^2\zeta^2)^{1/2} \times M_{L\varepsilon}(1-\zeta^2)^{1/2}\mathbf{PF}\left(\frac{1}{\cos^2\varphi-\zeta^2}\right)\mathrm{d}\zeta, \tag{87}$$

where

$$E(M_T,\varepsilon) = \frac{(2-M_T^2)^3}{\prod_{j=0}^{3}(M_T^2 - m_{j\varepsilon})}, \qquad N(M_T,\varepsilon) = \frac{4(2-M_T^2)}{\prod_{j=0}^{3}(M_T^2 - m_{j\varepsilon})}, \tag{88a, b}$$

with $m_{0\varepsilon} = 0$.

- Super-Rayleigh/subsonic range ($V_{R\varepsilon} < V < V_{\mathrm{T}}$):

$$u_z^{(Q)}(r,\varphi,z=0) = -\frac{Q\kappa h\cos\varphi}{(1+\varepsilon)^{1/2}\pi^2 r}\int_0^1 E^*(M_{\mathrm{T}}(1-\zeta^2)^{1/2},\varepsilon)M_{\mathrm{L}\varepsilon}(1-\zeta^2)^{1/2}\mathbf{PF}\left(\frac{1}{M_{\mathrm{T}}^2-m_{1\varepsilon}-M_{\mathrm{T}}^2\zeta^2}\right)$$
$$\times\,\mathbf{PF}\left(\frac{1}{\cos^2\varphi-\zeta^2}\right)\mathrm{d}\zeta - \frac{Q\kappa h\cos\varphi}{(1+\varepsilon)^{1/2}\pi^2 r}\int_0^1 N^*(M_{\mathrm{T}}(1-\zeta^2)^{1/2},\varepsilon)(1-M_{\mathrm{T}}^2+M_{\mathrm{T}}^2\zeta^2)^{1/2}$$
$$\times\,(1-M_{\mathrm{L}\varepsilon}^2+M_{\mathrm{L}\varepsilon}^2\zeta^2)^{1/2}M_{\mathrm{L}\varepsilon}(1-\zeta^2)^{1/2}\mathbf{PF}\left(\frac{1}{M_{\mathrm{T}}^2-m_{1\varepsilon}-M_{\mathrm{T}}^2\zeta^2}\right)\mathbf{PF}\left(\frac{1}{\cos^2\varphi-\zeta^2}\right)\mathrm{d}\zeta, \tag{89}$$

where

$$E^*(M_{\mathrm{T}},\varepsilon) = E(M_{\mathrm{T}},\varepsilon)(M_{\mathrm{T}}^2-m_{1\varepsilon}), \qquad N^*(M_{\mathrm{T}},\varepsilon) = N(M_{\mathrm{T}},\varepsilon)(M_{\mathrm{T}}^2-m_{1\varepsilon}). \tag{90a, b}$$

- Transonic range ($V_{\mathrm{T}} < V < V_{\mathrm{L}\varepsilon}$):

$$u_z^{(Q)}(r,\varphi,z=0) = \frac{Q\kappa h\sin\varphi}{2(1+\varepsilon)^{1/2}\pi r}N(M_{\mathrm{T}}\sin\varphi,\varepsilon)M_{\mathrm{L}\varepsilon}(1-M_{\mathrm{L}\varepsilon}^2\sin^2\varphi)^{1/2}(M_{\mathrm{T}}^2\sin^2\varphi-1)^{1/2}$$
$$\times\,H\left(|\sin\varphi|-\frac{1}{M_{\mathrm{T}}}\right) - \frac{Q\kappa h\cos\varphi}{(1+\varepsilon)^{1/2}\pi^2 r}\int_0^1 E^*(M_{\mathrm{T}}(1-\zeta^2)^{1/2},\varepsilon)M_{\mathrm{L}\varepsilon}(1-\zeta^2)^{1/2}$$
$$\times\,\mathbf{PF}\left(\frac{1}{M_{\mathrm{T}}^2-m_{1\varepsilon}-M_{\mathrm{T}}^2\zeta^2}\right)\mathbf{PF}\left(\frac{1}{\cos^2\varphi-\zeta^2}\right)\mathrm{d}\zeta - \frac{Q\kappa h\cos\varphi}{(1+\varepsilon)^{1/2}\pi^2 r}$$
$$\times\int_{[1-(1/M_{\mathrm{T}}^2)]^{1/2}}^1 N^*(M_{\mathrm{T}}(1-\zeta^2)^{1/2},\varepsilon)(1-M_{\mathrm{T}}^2+M_{\mathrm{T}}^2\zeta^2)^{1/2}(1-M_{\mathrm{L}\varepsilon}^2+M_{\mathrm{L}\varepsilon}^2\zeta^2)^{1/2}$$
$$\times\,M_{\mathrm{L}\varepsilon}(1-\zeta^2)^{1/2}\mathbf{PF}\left(\frac{1}{M_{\mathrm{T}}^2-m_{1\varepsilon}-M_{\mathrm{T}}^2\zeta^2}\right)\mathbf{PF}\left(\frac{1}{\cos^2\varphi-\zeta^2}\right)\mathrm{d}\zeta. \tag{91}$$

- Supersonic range ($V_{\mathrm{L}\varepsilon} < V$):

$$u_z^{(Q)}(r,\varphi,z=0) = \frac{Q\kappa h\sin\varphi}{2(1+\varepsilon)^{1/2}\pi r}N(M_{\mathrm{T}}\sin\varphi,\varepsilon)M_{\mathrm{L}\varepsilon}(1-M_{\mathrm{L}\varepsilon}^2\sin^2\varphi)^{1/2}(M_{\mathrm{T}}^2\sin^2\varphi-1)^{1/2}$$
$$\times\left[H\left(|\sin\varphi|-\frac{1}{M_{\mathrm{T}}}\right)-H\left(|\sin\varphi|-\frac{1}{M_{\mathrm{L}\varepsilon}}\right)\right] - \frac{Q\kappa h\cos\varphi}{(1+\varepsilon)^{1/2}\pi^2 r}\int_0^1 E^*(M_{\mathrm{T}}(1-\zeta^2)^{1/2},\varepsilon)$$
$$\times\,M_{\mathrm{L}\varepsilon}(1-\zeta^2)^{1/2}\mathbf{PF}\left(\frac{1}{M_{\mathrm{T}}^2-m_{1\varepsilon}-M_{\mathrm{T}}^2\zeta^2}\right)\mathbf{PF}\left(\frac{1}{\cos^2\varphi-\zeta^2}\right)\mathrm{d}\zeta + \frac{Q\kappa h\cos\varphi}{(1+\varepsilon)^{1/2}\pi^2 r}$$
$$\times\int_0^{[1-(1/M_{\mathrm{L}\varepsilon}^2)]^{1/2}} N(M_{\mathrm{T}}(1-\zeta^2)^{1/2},\varepsilon)(M_{\mathrm{T}}^2-M_{\mathrm{T}}^2\zeta^2-1)^{1/2}(M_{\mathrm{L}\varepsilon}^2-M_{\mathrm{L}\varepsilon}^2\zeta^2-1)^{1/2}$$
$$\times\,M_{\mathrm{L}\varepsilon}(1-\zeta^2)^{1/2}\mathbf{PF}\left(\frac{1}{\cos^2\varphi-\zeta^2}\right)\mathrm{d}\zeta - \frac{Q\kappa h\cos\varphi}{(1+\varepsilon)^{1/2}\pi^2 r}\int_{[1-(1/M_{\mathrm{T}}^2)]^{1/2}}^1 N^*(M_{\mathrm{T}}(1-\zeta^2)^{1/2},\varepsilon)$$
$$\times\,(1-M_{\mathrm{T}}^2+M_{\mathrm{T}}^2\zeta^2)^{1/2}(1-M_{\mathrm{L}\varepsilon}^2+M_{\mathrm{L}\varepsilon}^2\zeta^2)^{1/2}M_{\mathrm{L}\varepsilon}(1-\zeta^2)^{1/2}$$
$$\times\,\mathbf{PF}\left(\frac{1}{M_{\mathrm{T}}^2-m_{1\varepsilon}-M_{\mathrm{T}}^2\zeta^2}\right)\mathbf{PF}\left(\frac{1}{\cos^2\varphi-\zeta^2}\right)\mathrm{d}\zeta. \tag{92}$$

Nevertheless, in the case of poles at the points $\zeta = [1-(m_{j\varepsilon}/M_{\mathrm{T}}^2)]^{1/2}$, with ($j = 2, 3$), the first and the second integral, say I_3 and I_4, are written in the following forms that facilitate their numerical evaluation

$$I_3 = \sum_{j=0}^{3} E_j \int_0^1 \mathbf{PF}\left(\frac{1}{M_{\mathrm{T}}^2 - m_{j\varepsilon} - M_{\mathrm{T}}^2\zeta^2}\right)\mathbf{PF}\left(\frac{1}{\cos^2\varphi - \zeta^2}\right) M_{\mathrm{L}\varepsilon}(1-\zeta^2)^{1/2}\,\mathrm{d}\zeta, \tag{93}$$

$$I_4 = \sum_{j=0}^{3} N_j \int_0^{[1-(1/M_{\mathrm{L}\varepsilon}^2)]^{1/2}} \mathbf{PF}\left(\frac{1}{M_{\mathrm{T}}^2 - m_{j\varepsilon} - M_{\mathrm{T}}^2\zeta^2}\right)(M_{\mathrm{T}}^2 - M_{\mathrm{T}}^2\zeta^2 - 1)^{1/2}(M_{\mathrm{L}\varepsilon}^2 - M_{\mathrm{L}\varepsilon}^2\zeta^2 - 1)^{1/2} M_{\mathrm{L}\varepsilon}(1-\zeta^2)^{1/2} \times \mathbf{PF}\left(\frac{1}{\cos^2\varphi - \zeta^2}\right)\mathrm{d}\zeta, \tag{94}$$

where the constants E_j and N_j, with ($j = 0, 1, 2, 3, 4$), are defined in (A.15) and (A.16) of Appendix A. Again, these constants are expressed in terms of the non-trivial zeroes ($m_{1\varepsilon}, m_{2\varepsilon}, m_{3\varepsilon}$) of the function K_ε.

7. Additional results: tangential displacements

In general, the tangential displacements (u_x, u_y) can be found by operating with the inverse Radon transform in (10) on the transformed displacements $(\tilde{u}_x, \tilde{u}_y)$. The latter expressions result, of course, from (53) and the expressions for $(\tilde{u}_q, \tilde{u}_s)$. Then, the components (u_r, u_φ) in the cylindrical polar coordinate system may readily be obtained through the coordinate transformation (54). As before, the displacements will be obtained separately for the cases of vertical and tangential loading.

7.1. Tangential displacements due to the vertical load P

In this case, the solution to the first auxiliary problem is given by (37) and (40), whereas the solution to the second auxiliary problem is $\tilde{u}_s(q, \omega, z = 0) = 0$ since the boundary condition associated with (14) is $\tilde{\sigma}_{zs}(q, \omega, z = 0) = 0$. Accordingly, the following Radon transformed solutions are obtained

$$\tilde{u}_x^{(P)}(q, \omega, z = 0) = -\frac{P\mathrm{sgn}(\cos\omega)\cos\omega}{2\mu} G^{(P)}(M_{\mathrm{T}}\cos\omega, \varepsilon)\mathrm{sgn}(\mathrm{sqn}(\cos\omega)q), \tag{95}$$

$$\tilde{u}_y^{(P)}(q, \omega, z = 0) = -\frac{P\mathrm{sgn}(\cos\omega)\sin\omega}{2\mu} G^{(P)}(M_{\mathrm{T}}\cos\omega, \varepsilon)\mathrm{sgn}(\mathrm{sqn}(\cos\omega)q) \tag{96}$$

and further from (10), (55) and (59) and by the change of variable $\zeta = \sin\omega$, the tangential (horizontal) displacements are obtained as

$$u_x^{(P)}(r, \varphi, z = 0) = -\frac{P\cos\varphi}{\mu\pi^2 r}\int_0^1 G^{(P)}(M_{\mathrm{T}}(1-\zeta^2)^{1/2}, \varepsilon)(1-\zeta^2)^{1/2}\mathbf{PF}\left(\frac{1}{\cos^2\varphi - \zeta^2}\right)\mathrm{d}\zeta, \tag{97}$$

$$u_y^{(P)}(r, \varphi, z = 0) = \frac{P\sin\varphi}{\mu\pi^2 r}\int_0^1 G^{(P)}(M_{\mathrm{T}}(1-\zeta^2)^{1/2}, \varepsilon)\frac{\zeta^2}{(1-\zeta^2)^{1/2}}\mathbf{PF}\left(\frac{1}{\cos^2\varphi - \zeta^2}\right)\mathrm{d}\zeta, \tag{98}$$

where

$$G^{(P)}(M_{\mathrm{T}}(1-\zeta^2)^{1/2}, \varepsilon) = -C(M_{\mathrm{T}}(1-\zeta^2)^{1/2}, \varepsilon) - D(M_{\mathrm{T}}(1-\zeta^2)^{1/2}, \varepsilon) \times (1 - M_{\mathrm{T}}^2 + M_{\mathrm{T}}^2\zeta^2)^{1/2}(1 - M_{\mathrm{L}\varepsilon}^2 + M_{\mathrm{L}\varepsilon}^2\zeta^2)^{1/2}. \tag{99}$$

One may observe now that the expression for $u_x^{(P)}$ coincides with that for $u_z^{(S)}$, the latter being given by (77). This is not surprising in view of the dynamic version of the Betti–Rayleigh reciprocal theorem. Notice also that an opposite sign in the two expressions is due to the different direction of the loads w.r.t. the

corresponding displacements. In view of this observation, the analysis concerning $u_z^{(S)}$ in the subsonic range is carried over the case of $u_x^{(P)}$ as well. An inspection also on (97) and (98) reveals that both $u_x^{(P)}$ and $u_y^{(P)}$ do not exhibit thermoelastic Mach-type Rayleigh wavefronts. Eqs. (97) and (98) apply for both the sub-Rayleigh and super-Rayleigh/subsonic cases.

Finally, from (54), (97) and (98), the displacement components in a system of cylindrical polar coordinates (r, φ, z) (see Fig. 6) are found to be

$$u_r^{(P)}(r,\varphi,z=0) = -\frac{P}{\mu\pi^2 r}\int_0^1 G^{(P)}(M_T(1-\zeta^2)^{1/2},\varepsilon)\frac{1}{(1-\zeta^2)^{1/2}}\,\mathrm{d}\zeta, \tag{100}$$

$$u_\varphi^{(P)}(r,\varphi,z=0) = \frac{P\cos\varphi\sin\varphi}{\mu\pi^2 r}\int_0^1 G^{(P)}(M_T(1-\zeta^2)^{1/2},\varepsilon)\frac{1}{(1-\zeta^2)^{1/2}}\mathbf{PF}\left(\frac{1}{\cos^2\varphi-\zeta^2}\right)\mathrm{d}\zeta. \tag{101}$$

Eq. (100), in particular, shows that the radial displacement at the surface $u_r^{(P)}$ has no angular dependence. This result at first glance looks somewhat surprising but is in agreement with the respective result of the 'pure mechanical' case (Lansing, 1966; Georgiadis and Lykotrafitis, 2001). Also, the other component $u_\varphi^{(P)}$ is anti-symmetric w.r.t. both axes x and y, and vanishes along lines on the surface defined by the angles $\varphi = 0$, $\pi/2$, π, $3\pi/2$.

7.2. Tangential displacements due to the tangential load S

In this case, the second auxiliary problem does enter the 3D solution. Indeed, solutions (38) and (50) for $\tilde{\boldsymbol{u}}_q^{(S)}$ and $\tilde{\boldsymbol{u}}_s^{(S)}$, respectively, provide through (53) the Radon transformed displacements

$$\tilde{\boldsymbol{u}}_x^{(S)}(q,\omega,z=0) = -\frac{S}{\mu}[Q_1(M_T\cos\omega)\sin^2\omega - G^{(S)}(M_T\cos\omega,\varepsilon)\cos^2\omega]\ln(|q|), \tag{102}$$

$$\tilde{\boldsymbol{u}}_y^{(S)}(q,\omega,z=0) = \frac{S\cos\omega\sin\omega}{\mu}[Q_1(M_T\cos\omega) + G^{(S)}(M_T\cos\omega,\varepsilon)]\ln(|q|), \tag{103}$$

where the functions of the Mach number M_T, $G^{(S)}(M_T,\varepsilon)$ and $Q_1(M_T)$ are given in (41) and (51), respectively. Then, combining the latter equations and (10), (56) and (59) leads to the tangential displacements in the subsonic range

$$u_x^{(S)}(r,\varphi,z=0) = \frac{S}{2\mu r}[Q_{11}(M_T\sin\varphi)\cos^2\varphi - G^{(S)}(M_T\sin\varphi,\varepsilon)\sin^2\varphi], \tag{104}$$

$$u_y^{(S)}(r,\varphi,z=0) = \frac{S\cos\varphi\sin\varphi}{2\mu r}[Q_{11}(M_T\sin\varphi) + G^{(S)}(M_T\sin\varphi,\varepsilon)]. \tag{105}$$

In addition, applying (54) to (104) and (105) yields

$$u_r^{(S)}(r,\varphi,z=0) = \frac{S\cos\varphi}{2\mu r}Q_{11}(M_T\sin\varphi), \tag{106}$$

$$u_\varphi^{(S)}(r,\varphi,z=0) = \frac{S\sin\varphi}{2\mu r}G^{(S)}(M_T\sin\varphi,\varepsilon). \tag{107}$$

Below, the sub-Rayleigh and the super-Rayleigh/subsonic cases will be treated separately.

- Sub-Rayleigh range ($0 < V < V_{Re}$):

Here, the displacements can be calculated from (104)–(107). It is of notice that $u_x^{(S)}$ and $u_y^{(S)}$ are symmetric and anti-symmetric, respectively, w.r.t. both axes x and y.

- Super-Rayleigh subsonic range ($V_{R\varepsilon} < V < V_T$):

In this case, solutions (104) and (105) exhibit singular behavior along the Rayleigh wavefronts, where $R(M_T \sin\varphi) = 0$. In this form, the solutions give *two* Rayleigh sectors; one ahead of the load S and the other behind. Since only trailing Rayleigh waves are acceptable by the radiation condition, the sector ahead of the load should be eliminated. Following the same reasoning as in the respective case of $u_z^{(P)}$ (see Section 6.1), we write the *corrected* solutions as

$$u_x^{(S)}(r,\varphi,z=0) = \frac{S}{2\mu}\left[\frac{1}{r}Q_{11}(M_T\sin\varphi)\cos^2\varphi - G^{(S)}(M_T\sin\varphi,\varepsilon)\sin^2\varphi + \frac{\Phi}{r\sin(\varphi-\varphi_{R\varepsilon})} - \frac{\Phi}{r\sin(\varphi+\varphi_{R\varepsilon})}\right], \tag{108}$$

$$u_y^{(S)}(r,\varphi,z=0) = \frac{S\cos\varphi\sin\varphi}{2\mu}\left[\frac{1}{r}Q_{11}(M_T\sin\varphi) + G^{(S)}(M_T\sin\varphi,\varepsilon) + \frac{\Psi}{r\sin(\varphi-\varphi_{R\varepsilon})} + \frac{\Psi}{r\sin(\varphi+\varphi_{R\varepsilon})}\right], \tag{109}$$

where the constants Φ and Ψ are determined by imposing the elimination of the leading Rayleigh-wave sectors. The final expressions read

$$u_x^{(S)}(r,\varphi,z=0) = \frac{S}{2\mu r}\left[Q_{11}(M_T\sin\varphi)\cos^2\varphi - G^{(S)}(M_T\sin\varphi,\varepsilon)\sin^2\varphi + \frac{\cos\varphi m_{1\varepsilon}(1-m_{1\varepsilon})^{1/2}[(2-m_{1\varepsilon})^2 + 4(1-m_{1\varepsilon})^{1/2}(1-m_\varepsilon^{-2}m_{1\varepsilon})^{1/2}]}{\pi M_T(M_T^2\sin^2\varphi - m_{1\varepsilon})(M_T^2 - m_{1\varepsilon})^{1/2}(m_{1\varepsilon}-m_{2\varepsilon})(m_{1\varepsilon}-m_{3\varepsilon})}\right], \tag{110}$$

$$u_y^{(S)}(r,\varphi,z=0) = \frac{S\cos\varphi\sin\varphi}{2\mu r}\left[Q_{11}(M_T\sin\varphi) + G^{(S)}(M_T\sin\varphi,\varepsilon) - \frac{(M_T^2-m_{1\varepsilon})^{1/2}(1-m_{1\varepsilon})^{1/2}[(2-m_{1\varepsilon})^2 + 4(1-m_{1\varepsilon})^{1/2}(1-m_\varepsilon^{-2}m_{1\varepsilon})^{1/2}]}{\pi\cos\varphi M_T(M_T^2\sin^2\varphi - m_{1\varepsilon})(m_{1\varepsilon}-m_{2\varepsilon})(m_{1\varepsilon}-m_{3\varepsilon})}\right]. \tag{111}$$

Finally, operating with the transformation (54) on (110) and (111) provides the displacement components

$$u_r^{(S)}(r,\varphi,z=0) = \frac{S}{2\mu r}\left[Q_{11}(M_T\sin\varphi)\cos\varphi - \frac{(1-m_{1\varepsilon})^{1/2}[(2-m_{1\varepsilon})^2 + 4(1-m_{1\varepsilon})^{1/2}(1-m_\varepsilon^{-2}m_{1\varepsilon})^{1/2}]}{\pi M_T(M_T^2 - m_{1\varepsilon})^{1/2}(m_{1\varepsilon}-m_{2\varepsilon})(m_{1\varepsilon}-m_{3\varepsilon})}\right], \tag{112}$$

$$u_\varphi^{(S)}(r,\varphi,z=0) = \frac{S\sin\varphi}{2\mu r}\left[G^{(S)}(M_T\sin\varphi,\varepsilon) - \frac{\cos\varphi M_T(1-m_1)^{1/2}[(2-m_{1\varepsilon})^2 + 4(1-m_{1\varepsilon})^{1/2}(1-m_\varepsilon^{-2}m_{1\varepsilon})^{1/2}]}{\pi(M_T^2\sin^2\varphi - m_{1\varepsilon})(M_T^2 - m_{1\varepsilon})^{1/2}(m_{1\varepsilon}-m_{2\varepsilon})(m_{1\varepsilon}-m_{3\varepsilon})}\right], \tag{113}$$

where it is noticed that thermoelastic Rayleigh Mach-type wavefronts do not exist for $u_r^{(S)}$ and also that $u_\varphi^{(S)}$ is anti-symmetric w.r.t. the x-axis.

7.3. Tangential displacements due to the heat source KQ

The appropriate solution to the first auxiliary problem is given by (39) and (42), whereas the second auxiliary problem does not play a role in view of the boundary condition $\tilde{\boldsymbol{u}}_s(q,\omega,z=0)=0$ that accompanies the PDE in (14) (this is expected, of course, since a thermal field does not interfere with shear waves in coupled thermoelasticity). The Radon transformed solution is now obtained from the aforementioned auxiliary solution through the coordinate transformation (53)

$$\tilde{u}_x^{(Q)}(q,\omega,z=0)=\frac{Q\kappa h}{(1+\varepsilon)^{1/2}}G^{(Q)}(M_{\mathrm{T}}\cos\omega,\varepsilon)\cos\omega\ln(|q|), \tag{114}$$

$$\tilde{u}_y^{(Q)}(q,\omega,z=0)=\frac{Q\kappa h}{(1+\varepsilon)^{1/2}}G^{(Q)}(M_{\mathrm{T}}\cos\omega,\varepsilon)\sin\omega\ln(|q|). \tag{115}$$

Further, by the standard inversion procedure, we obtain the following basic results for the horizontal displacement components $(u_x^{(Q)},u_y^{(Q)})$ in the Cartesian system and $(u_r^{(Q)},u_\varphi^{(Q)})$ in the cylindrical polar system. Both pairs of components, however, are expressed for convenience in terms of the coordinates (r,φ)

$$u_x^{(Q)}(r,\varphi,z=0)=-\frac{Q\kappa h\sin\varphi}{2(1+\varepsilon)^{1/2}r}G^{(Q)}(M_{\mathrm{T}}\sin\varphi,\varepsilon), \tag{116}$$

$$u_y^{(Q)}(r,\varphi,z=0)=\frac{Q\kappa h\cos\varphi}{2(1+\varepsilon)^{1/2}r}G^{(Q)}(M_{\mathrm{T}}\sin\varphi,\varepsilon), \tag{117}$$

$$u_r^{(Q)}(r,\varphi,z=0)=0, \tag{118}$$

$$u_\varphi^{(Q)}(r,\varphi,z=0)=\frac{Q\kappa h}{2(1+\varepsilon)^{1/2}r}G^{(Q)}(M_{\mathrm{T}}\sin\varphi,\varepsilon). \tag{119}$$

From the above expressions, particular results will be extracted for the sub-Rayleigh and the super-Rayleigh/subsonic velocity regimes.

- Sub-Rayleigh range $(0<V<V_R)$:

In this case, relations (116)–(119) need no modification. It is noticed that $u_x^{(Q)}$ is symmetric w.r.t. both axes x and y, whereas $u_y^{(Q)}$ is anti-symmetric.

- Super-Rayleigh/subsonic range $(V_R<V<V_{\mathrm{T}})$:

In this case, the solution in (116) and (117) exhibits both leading and trailing Rayleigh sectors. Of course, the former sector should be eliminated and by the usual procedure the following result is found

$$\begin{aligned}u_x^{(Q)}(r,\varphi,z=0)=-\frac{Q\kappa h}{2(1+\varepsilon)^{1/2}r}\Bigg[&G^{(Q)}(M_{\mathrm{T}}\sin\varphi,\varepsilon)\sin\varphi\\&+\frac{2\cos\varphi m_\varepsilon^{-1}[(2-m_{1\varepsilon})^2(1-m_{1\varepsilon})^{1/2}+4(1-m_{1\varepsilon})(1-m_\varepsilon^{-2}m_{1\varepsilon})^{1/2}]}{\pi(M_{\mathrm{T}}^2\sin^2\varphi-m_{1\varepsilon})(M_{\mathrm{T}}^2-m_{1\varepsilon})^{1/2}(m_{1\varepsilon}-m_{2\varepsilon})(m_{1\varepsilon}-m_{3\varepsilon})}\Bigg],\end{aligned} \tag{120}$$

$$\begin{aligned}u_y^{(Q)}(r,\varphi,z=0)=\frac{Q\kappa h\cos\varphi}{2(1+\varepsilon)^{1/2}r}\Bigg[&G^{(Q)}(M_{\mathrm{T}}\sin\varphi,\varepsilon)\\&+\frac{2\sin\varphi m_\varepsilon^{-1}(M_{\mathrm{T}}^2-m_{1\varepsilon})^{1/2}[(2-m_{1\varepsilon})^2(1-m_{1\varepsilon})^{1/2}+4(1-m_{1\varepsilon})(1-m_\varepsilon^{-2}m_{1\varepsilon})^{1/2}]}{\pi\cos\varphi(M_{\mathrm{T}}^2\sin^2\varphi-m_{1\varepsilon})m_{1\varepsilon}(m_{1\varepsilon}-m_{2\varepsilon})(m_{1\varepsilon}-m_{3\varepsilon})}\Bigg],\end{aligned} \tag{121}$$

$$u_r^{(Q)}(r,z=0)=\frac{Q\kappa h}{(1+\varepsilon)^{1/2}\pi r}\,\frac{m_\varepsilon^{-1}[(2-m_{1\varepsilon})^2(1-m_{1\varepsilon})^{1/2}+4(1-m_{1\varepsilon})(1-m_\varepsilon^{-2}m_{1\varepsilon})^{1/2}]}{m_{1\varepsilon}(m_{1\varepsilon}-m_{2\varepsilon})(m_{1\varepsilon}-m_{3\varepsilon})(M_{\mathrm{T}}^2-m_{1\varepsilon})^{1/2}}, \tag{122}$$

$$u_\varphi^{(Q)}(r,\varphi,z=0)=\frac{Q\kappa h}{2(1+\varepsilon)^{1/2}r}\left[G^{(Q)}(M_{\mathrm{T}}\sin\varphi,\varepsilon)+\frac{2m_\varepsilon^{-1}M_{\mathrm{T}}^2\sin\varphi\cos\varphi[(2-m_{1\varepsilon})^2(1-m_{1\varepsilon})^{1/2}+4(1-m_{1\varepsilon})(1-m_\varepsilon^{-2}m_{1\varepsilon})^{1/2}]}{\pi(M_{\mathrm{T}}^2-m_{1\varepsilon})^{1/2}(M_{\mathrm{T}}^2\sin^2\varphi-m_{1\varepsilon})m_{1\varepsilon}(m_{1\varepsilon}-m_{2\varepsilon})(m_{1\varepsilon}-m_{3\varepsilon})}\right]. \tag{123}$$

8. Change in temperature

8.1. Change in temperature due to the normal load P

Operating with the inverse Radon transform on (44), one obtains

$$\begin{aligned}\theta^{(P)}(r,\varphi,z=0)&=-\frac{P\varepsilon}{4\pi^2\mu\kappa(1+\varepsilon)}\left\{\int_0^{2\pi}\left[\frac{L_1^{(P)}(M_{\mathrm{T}}\cos\omega,\varepsilon)}{\operatorname{sgn}(\cos\omega)}\left(\int_{-\infty}^{+\infty}\frac{\mathrm{d}[\mathbf{PF}(q^{-1})]}{\mathrm{d}q}\mathbf{PF}\left(\frac{1}{q-r\cos(\omega-\varphi)}\right)\mathrm{d}q\right)\right]\mathrm{d}\omega\right.\\&\left.+\int_0^{2\pi}\left[L_2^{(P)}(M_{\mathrm{T}}\cos\omega,\varepsilon)\left(\int_{-\infty}^{+\infty}\frac{\mathrm{d}\delta(q)}{\mathrm{d}q}\mathbf{PF}\left(\frac{1}{q-r\cos(\omega-\varphi)}\right)\mathrm{d}q\right)\right]\mathrm{d}\omega\right\}.\end{aligned} \tag{124}$$

The evaluation now of the two inner integrals in (124) is accomplished by utilizing the following distributional properties involving differentiation of convolutions (Gel'fand and Shilov, 1964; Roos, 1969)

$$\int_{-\infty}^{+\infty}\frac{\mathrm{d}[\mathbf{PF}(q^{-1})]}{\mathrm{d}q}\mathbf{PF}\left(\frac{1}{q-a}\right)\mathrm{d}q=\frac{\mathrm{d}}{\mathrm{d}a}\left[\int_{-\infty}^{+\infty}\mathbf{PF}\left(\frac{1}{q}\right)\mathbf{PF}\left(\frac{1}{q-a}\right)\mathrm{d}q\right]=\pi^2\frac{\mathrm{d}\delta(a)}{\mathrm{d}a}, \tag{125}$$

$$\int_{-\infty}^{+\infty}\frac{\mathrm{d}\delta(q)}{\mathrm{d}q}\mathbf{PF}\left(\frac{1}{q-a}\right)\mathrm{d}q=\frac{\mathrm{d}}{\mathrm{d}a}\left[\int_{-\infty}^{+\infty}\delta(q)\mathbf{PF}\left(\frac{1}{q-a}\right)\mathrm{d}q\right]=\frac{\mathrm{d}[\mathbf{PF}(-a^{-1})]}{\mathrm{d}a}. \tag{126}$$

With the above results in hand, Eq. (124) becomes

$$\begin{aligned}\theta^{(P)}(r,\varphi,z=0)=-\frac{P\varepsilon}{4\mu\kappa(1+\varepsilon)}&\left\{\int_0^{2\pi}\frac{L_1^{(P)}(M_{\mathrm{T}}\cos\omega,\varepsilon)}{\operatorname{sgn}(\cos\omega)}\frac{\mathrm{d}[\delta(r\cos(\omega-\varphi))]}{\mathrm{d}[r\cos(\omega-\varphi)]}\mathrm{d}\omega\right.\\&\left.+\int_0^{2\pi}L_2^{(P)}(M_{\mathrm{T}}\cos\omega,\varepsilon)\frac{\mathrm{d}[\mathbf{PF}(-[r\cos(\omega-\varphi)]^{-1})]}{\mathrm{d}[r\cos(\omega-\varphi)]}\mathrm{d}\omega\right\}.\end{aligned} \tag{127}$$

Next, the two integrals in (127) will be evaluated by using again distribution theory. More specifically, for the first integral we rely upon the following results. First, let $f(t)$ be a real-valued function, which is twice continuously differentiable and varies *monotonically* from $f(a)$ to $f(b)$ as t increases from a to b, and also $f(c)=0$ with $a<c<b$. Then, it is valid that (Hoskins, 1979)

$$\frac{\mathrm{d}\delta[f(t)]}{\mathrm{d}f(t)}=\frac{1}{|f'(c)|^2}\left\{\frac{\mathrm{d}\delta(t-c)}{\mathrm{d}t}+\frac{f''(c)}{f'(c)}\delta(t-c)\right\}$$

if $f(t)$ increases in the considered interval, whereas

$$\frac{\mathrm{d}\delta[f(t)]}{\mathrm{d}f(t)} = -\frac{1}{|f'(c)|^2}\left\{\frac{\mathrm{d}\delta(t-c)}{\mathrm{d}t} + \frac{f''(c)}{f'(c)}\delta(t-c)\right\}$$

if $f(t)$ decreases in the same interval. Secondly, use is made of the definition of the derivative of the Dirac delta distribution, i.e.

$$\int_{-\infty}^{+\infty} f(\zeta)\delta'(\zeta)\,\mathrm{d}\zeta = -f'(0).$$

These two properties along with the observation that $L_1^{(P)}(M_\mathrm{T}\sin\varphi,\varepsilon)\cos\varphi\delta(\sin\varphi) = 0$ (this is because $L_1^{(P)}(0,\varepsilon) = 0$), lead to the result

$$\frac{2\pi^2}{r^2\mathrm{sgn}(-\sin\varphi)}\left\{\frac{\mathrm{d}[L_1^{(P)}(M_\mathrm{T}\cos(\omega+\varphi),\varepsilon)]}{\mathrm{d}\omega}\right\}_{\omega=\pi/2}$$

for the first integral. As for the second integral, we first apply the change of variable $\zeta = \cos\omega$ and then make use of the distributional property $\mathrm{d}\{\mathbf{PF}(q^{-1})\}/\mathrm{d}q = -\mathbf{PF}(q^{-2})$. In view of the above, Eq. (127) becomes

$$\theta^{(P)}(r,\varphi,z=0) = -\frac{P\varepsilon}{2\pi^2\mu\kappa(1+\varepsilon)r^2}\left\{\frac{\pi^2}{\mathrm{sgn}(-\sin\varphi)}\frac{\mathrm{d}[L_1^{(P)}(M_\mathrm{T}\cos(\omega+\varphi),\varepsilon)]}{\mathrm{d}\omega}\bigg|_{\omega=\pi/2} + \int_0^1 \frac{L_2^{(P)}[M_\mathrm{T}f(\zeta),\varepsilon]}{(1-\zeta^2)^{1/2}}\mathbf{PF}\left(\frac{1}{\zeta^2}\right)\mathrm{d}\zeta + \int_0^1 \frac{L_2^{(P)}[M_\mathrm{T}g(\zeta),\varepsilon]}{(1-\zeta^2)^{1/2}}\mathbf{PF}\left(\frac{1}{\zeta^2}\right)\mathrm{d}\zeta\right\}, \tag{128}$$

where $f(\zeta) = \zeta\cos\varphi + (1-\zeta^2)^{1/2}\sin\varphi$ and $g(\zeta) = \zeta\cos\varphi - (1-\zeta^2)^{1/2}\sin\varphi$.

8.2. Change in temperature due to the tangential load S

Operating with the inverse Radon transform on (45) and proceeding along the same lines as in the previous case, we obtain the final result

$$\theta^{(S)}(r,\varphi,z=0) = -\frac{S\varepsilon}{2\pi^2\mu\kappa(1+\varepsilon)r^2} \times\left\{-\pi^2\left[\frac{\mathrm{d}[L_1^{(P)}(M_\mathrm{T}\cos(\omega+\varphi),\varepsilon)]}{\mathrm{d}\omega}\bigg|_{\omega=\pi/2}\sin\varphi + L_1^{(P)}(M_\mathrm{T}\sin\varphi,\varepsilon)\cos\varphi\right] + \int_0^1 \frac{L_2^{(S)}[M_\mathrm{T}f(\zeta),\varepsilon]|f(\zeta)|}{(1-\zeta^2)^{1/2}}\mathbf{PF}\left(\frac{1}{\zeta^2}\right)\mathrm{d}\zeta + \int_0^1 \frac{L_2^{(S)}[M_\mathrm{T}g(\zeta),\varepsilon]|g(\zeta)|}{(1-\zeta^2)^{1/2}}\mathbf{PF}\left(\frac{1}{\zeta^2}\right)\mathrm{d}\zeta\right\}. \tag{129}$$

9. Numerical results

The numerical results are presented in the form of graphs showing the normalized dimensionless displacements $U_z^{(P)} = u_z^{(P)}\mu r/P$, $U_z^{(S)} = u_z^{(S)}\mu r/S$, $U_z^{(Q)} = u_z^{(Q)}(1+\varepsilon)^{1/2}r/\kappa Qh$, $U_r^{(P)} = u_r^{(P)}\mu r/P$, $U_r^{(S)} = u_r^{(S)}\mu r/S$, $U_r^{(Q)} = u_r^{(Q)}(1+\varepsilon)^{1/2}r/\kappa Qh$, $U_\varphi^{(P)} = u_\varphi^{(P)}\mu r/P$, $U_\varphi^{(S)} = u_\varphi^{(S)}\mu r/S$ and $U_\varphi^{(Q)} = u_\varphi^{(Q)}(1+\varepsilon)^{1/2}r/\kappa Qh$ as functions of

the polar angle φ or the shear Mach number M_T, for a material with Poisson's ratio $v = 0.3$ and thermoelastic coupling constant $\varepsilon = 0.011$. All integrals appearing in the results of Sections 6–8 were evaluated numerically.

Fig. 8 shows $U_z^{(P)}$ vs. φ curves for various load speeds. In the sub-Rayleigh range (case of $M_T = 0.8$) the displacement is positive and, therefore, is directed into the half space. In the subsonic/super-Rayleigh range (case of $M_T = 0.95$), there is a Cauchy-type discontinuity along the Rayleigh Mach wavefronts at $\varphi = 106.47°$ and the displacement is positive in the sector defined by the Rayleigh lines (behind the load) but negative elsewhere. In the transonic range (case of $M_T = 1.2$), there is a Cauchy-type discontinuity along the Rayleigh wavefronts at $\varphi = 130.61°$ and a slope discontinuity along the shear wavefronts (defined by $M_T^2 \sin^2 \varphi = 1$) at $\varphi = 123.56°$. In the supersonic range (case of $M_T = 2.5$), the displacement suffers a Cauchy-type discontinuity along the Rayleigh wavefronts at $\varphi = 158.63°$ and a slope discontinuity along the shear wavefronts at $\varphi = 156.42°$. In the same range, the displacement becomes zero along the longitudinal wavefronts at $\varphi = 139.22°$.

Figs. 9–12 show $U_z^{(S)}$ vs. φ curves for, respectively, a sub-Rayleigh speed of the load S ($M_T = 0.8$), a super-Rayleigh/subsonic speed ($M_T = 0.95$), a transonic speed ($M_T = 1.2$) and a supersonic speed ($M_T = 2.5$). It is of notice in the super-Rayleigh/subsonic case that $U_z^{(S)}$ is continuous along the Rayleigh lines at $\varphi = 106.47°$ and that the magnitude of $U_z^{(S)}$ is smaller (by a factor of 10, approximately) in the super-Rayleigh case as compared to that in the sub-Rayleigh case. Also $U_z^{(S)}$ is symmetric w.r.t. the x-axis and is zero along lines at $\varphi = \pi/2, 3\pi/2$. In the transonic case, $U_z^{(S)}$ experiences a slope discontinuity at the shear Mach wavefronts and, also, it is negative inside the shear wavefront sector but positive outside this sector. Finally, Fig. 12 shows that $U_z^{(S)}$, in the supersonic case, is zero everywhere except in the region of the two sectors between the longitudinal and shear wavefront lines.

Fig. 13 shows the variation of $U_r^{(P)}$ with the Mach number M_T in the subsonic range, where $U_r^{(P)}$ is independent of the polar angle φ. The radial displacement is negative (i.e. its direction is towards the point of application of the load) and becomes infinite as the velocity approaches the Rayleigh wave velocity at

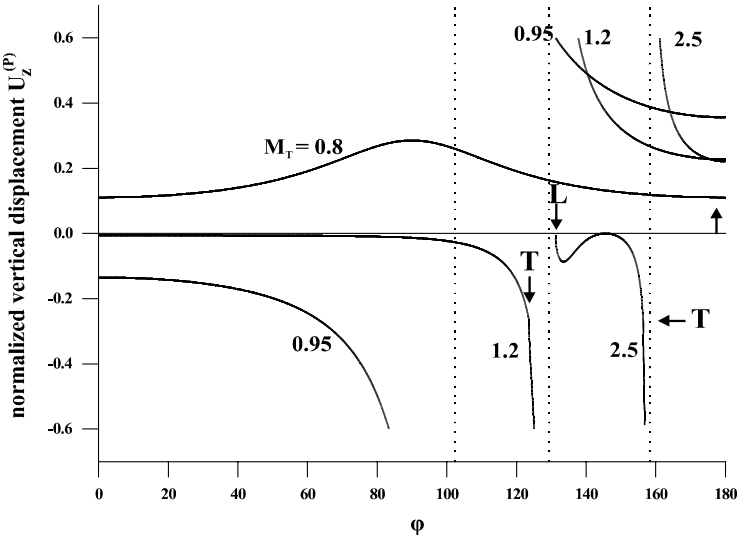

Fig. 8. Variation of the normalized vertical displacement $U_z^{(P)} = u_z^{(P)} \mu r/P$, due to a normal moving load, with the polar angle φ for various load speeds (cases of $M_T = 0.8$, 0.95, 1.2 and 2.5, which correspond to sub-Rayleigh, super-Rayleigh/subsonic, transonic and supersonic motion, respectively). The symbols L and T mark discontinuities associated with longitudinal and transverse (shear) wavefronts, respectively.

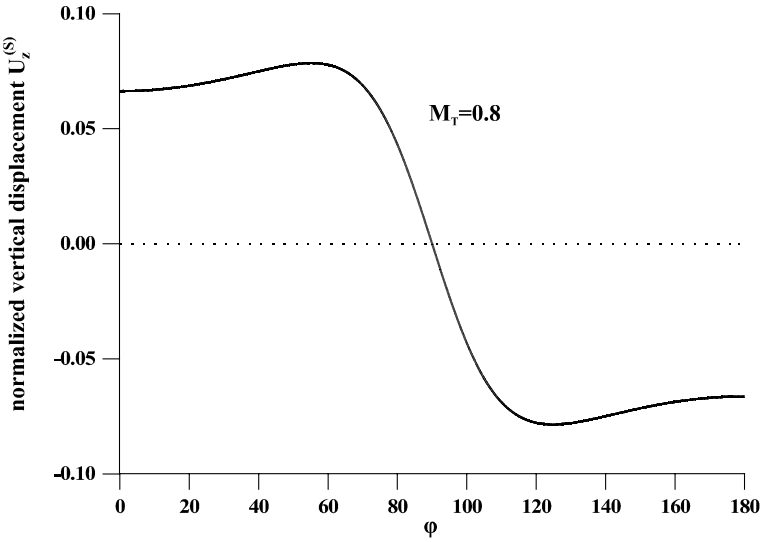

Fig. 9. Variation of the normalized vertical displacement $U_z^{(S)} = u_z^{(S)}\mu r/S$, due to a tangential moving load, with the polar angle φ for a load speed $M_T = 0.8$.

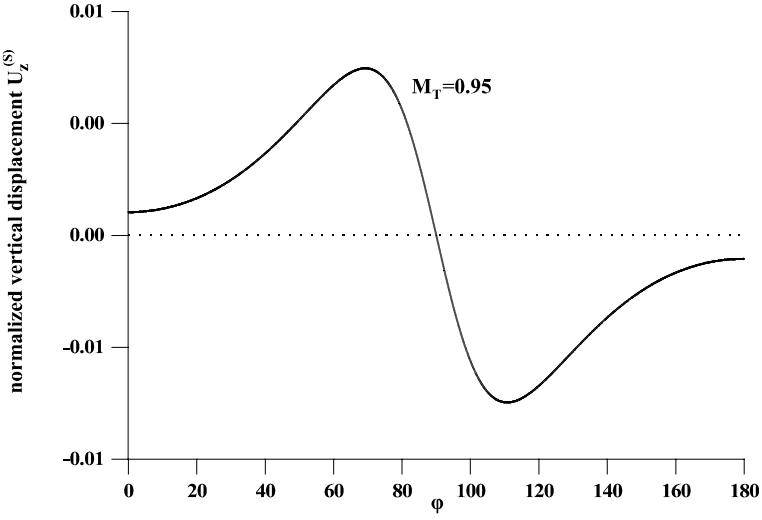

Fig. 10. Variation of the normalized vertical displacement $U_z^{(S)} = u_z^{(S)}\mu r/S$, due to a tangential moving load, with the polar angle φ for a load speed $M_T = 0.95$.

$V_R/V_T \cong 0.91$. At this speed the displacement is discontinuous. When $V_R < V$, $U_r^{(P)}$ is finite everywhere and remains continuous across the Rayleigh lines. Fig. 14 shows the variation of $U_r^{(P)}$ with φ indicating that this displacement component is continuous across the Rayleigh lines, the x-axis and the y-axis. $U_r^{(P)}$ is anti-symmetric w.r.t. the x and y axes. Also, one may observe that the magnitude of $U_r^{(P)}$ is much smaller in the super-Rayleigh speed (case of $M_T = 0.95$) than the one in the sub-Rayleigh speed (case of $M_T = 0.8$).

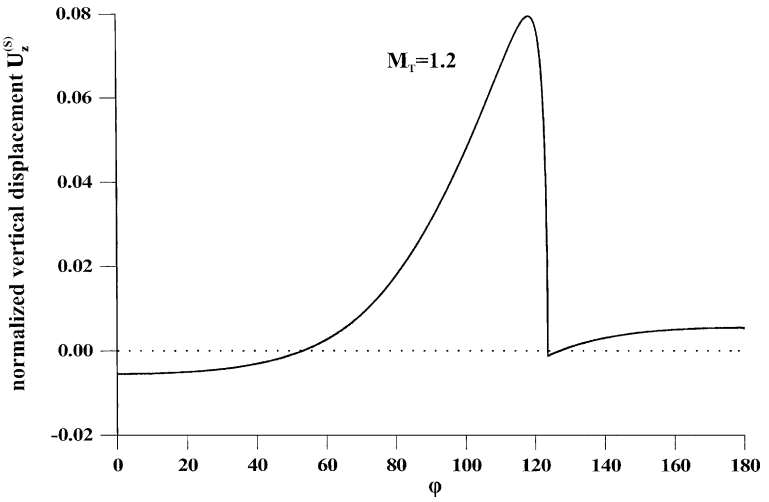

Fig. 11. Variation of the normalized vertical displacement $U_z^{(S)} = u_z^{(S)}\mu r/S$, due to a tangential moving load, with the polar angle φ for a load speed $M_T = 1.2$.

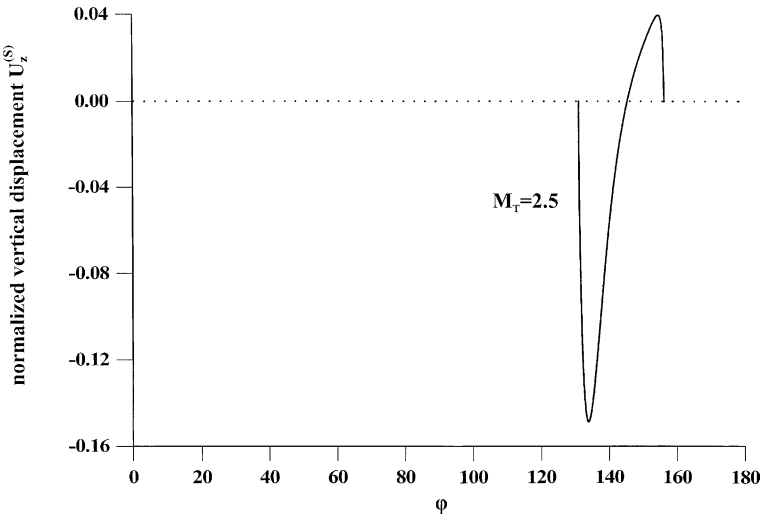

Fig. 12. Variation of the normalized vertical displacement $U_z^{(S)} = u_z^{(S)}\mu r/S$, due to a tangential moving load, with the polar angle φ for a load speed $M_T = 2.5$.

Fig. 15 shows the variation of $U_r^{(S)}$ with φ at load velocities $M_T = 0.8$ and 0.95. No Rayleigh singularity appears and $U_r^{(S)}$ is continuous and bounded in all directions. Fig. 16 depicts $U_\varphi^{(S)}$ vs. φ indicating that this displacement component: (i) is continuous in the entire φ range, (ii) is negative in the half-plane $y > 0$ and positive in the half-plane $y < 0$, in the case of sub-Rayleigh speeds ($M_T = 0.8$), and (iii) suffers a Cauchy-type singularity at the Rayleigh wavefront, in the case of super-Rayleigh speeds ($M_T = 0.95$).

A qualitative comparison of the present results with the respective results for the 'pure mechanical' problem (Georgiadis and Lykotrafitis, 2001) shows generally that the variation of the displacements is

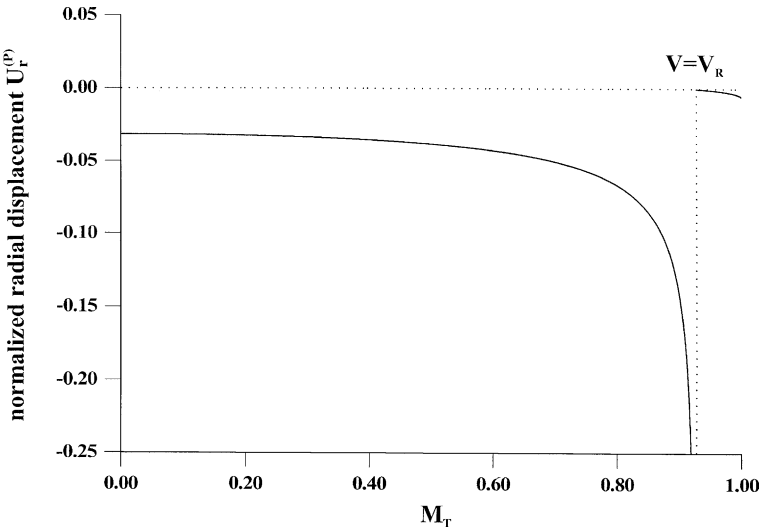

Fig. 13. Variation of the normalized radial displacement $U_r^{(P)} = u_r^{(P)}\mu r/P$, due to a normal moving load, with the transverse Mach number M_T. The discontinuity occurs when the load speed reaches the thermoelastic Rayleigh-wave speed in the medium.

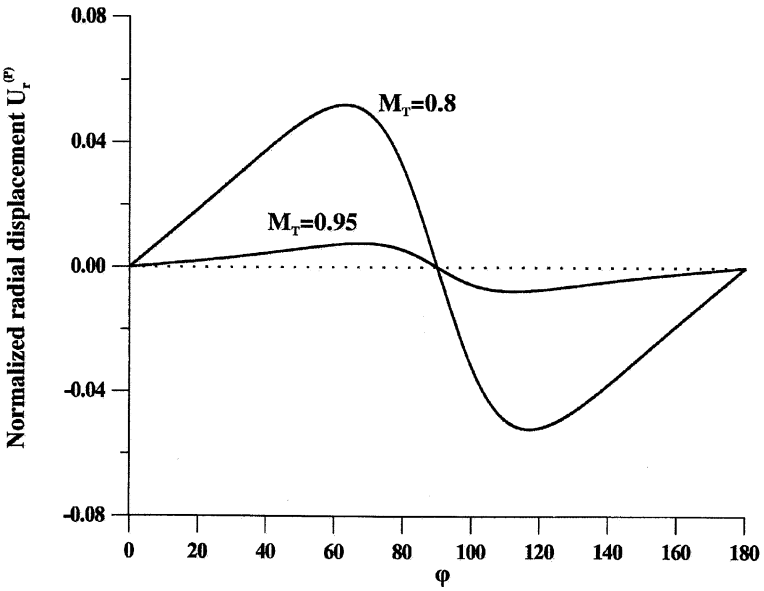

Fig. 14. Variation of the normalized radial displacement $U_r^{(P)} = u_r^{(P)}\mu r/P$, due to a normal moving load, with the polar angle φ for load speeds $M_T = 0.8$ and 0.95.

smoother in the thermoelastic case. This can be attributed to the diffusive components in the governing equations.

As for the thermal source, Figs. 17–20 present the variation of $U_z^{(Q)}$ with φ for the source velocities $M_T = 0.8$, 0.95, 1.2 and 2.5. These results show the occurrence of singularities along the line of motion of the thermal source (i.e. ahead of and behind the source). Also, as the source speed increases in the subsonic

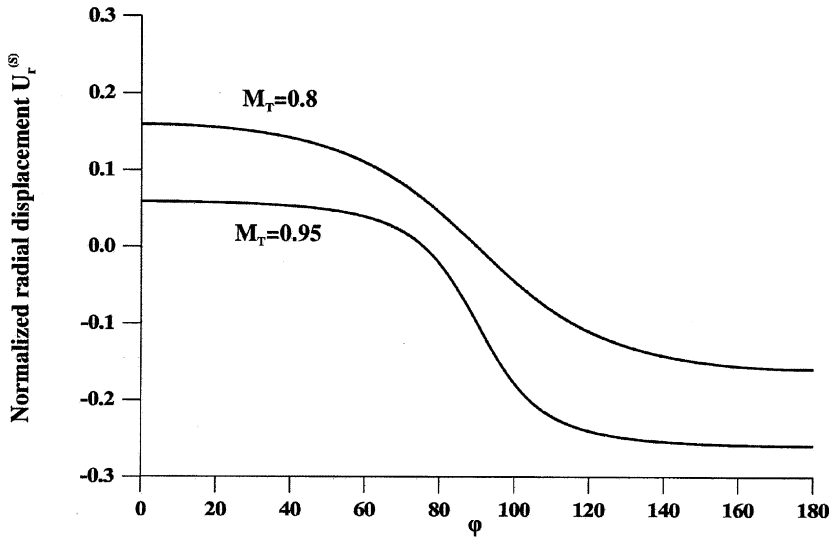

Fig. 15. Variation of the normalized radial displacement $U_r^{(S)} = u_r^{(S)}\mu r/S$, due to a tangential moving load, with the polar angle φ for load speeds $M_T = 0.8$ and 0.95.

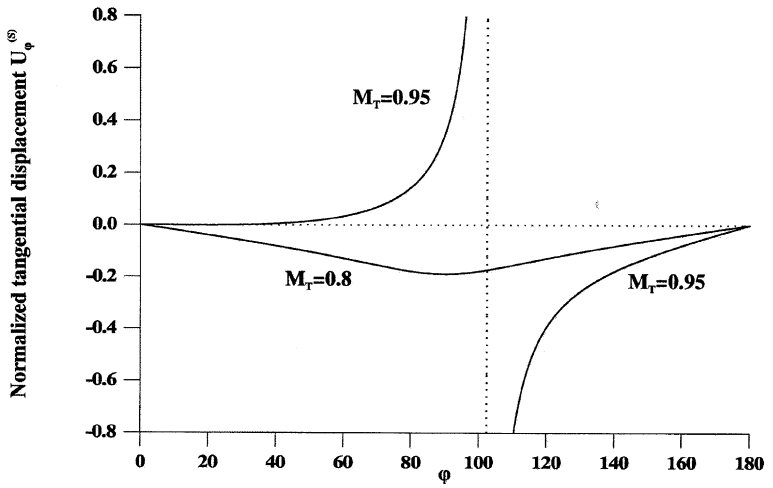

Fig. 16. Variation of the normalized tangential displacement $U_\varphi^{(S)} = u_\varphi^{(S)}\mu r/S$, due to a tangential moving load, with the polar angle φ for $M_T = 0.8$ and 0.95.

regime (results presented in Figs. 17 and 18) the vertical displacement decreases. An analogous result was detected in the results given before for the case of a mechanical source. In Figs. 19 and 20 discontinuities appear along the transverse and longitudinal wavefronts, respectively. In addition, Fig. 21 shows the variation of $U_r^{(Q)}$ with the shear Mach number M_T in the subsonic regime. A comparison between the $U_r^{(Q)}$ vs. M_T behavior (Fig. 21) and the $U_r^{(P)}$ vs. M_T behavior (Fig. 13) contrasts the difference between the action of moving thermal and point-load sources. Indeed, in the case of a thermal source, $U_r^{(Q)} = 0$ in the whole

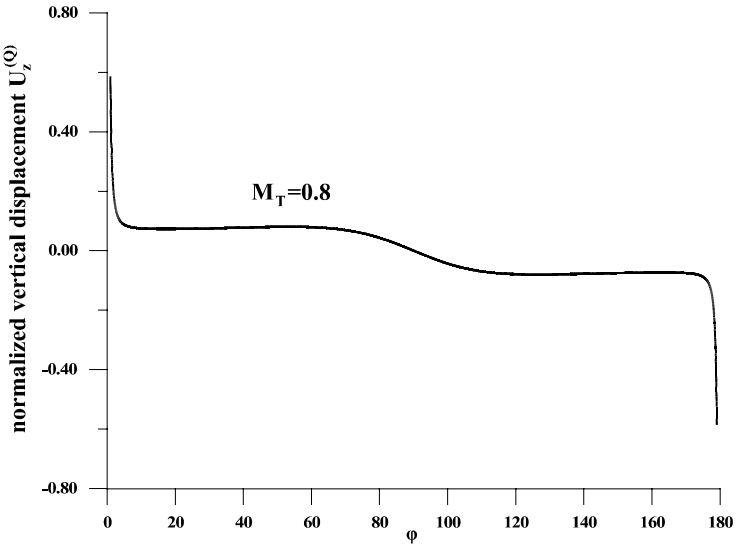

Fig. 17. Variation of the normalized vertical displacement $U_z^{(Q)} = u_z^{(Q)}(1+\varepsilon)^{1/2} r/\kappa Q h$, due to a thermal moving load, with the polar angle φ for $M_T = 0.8$.

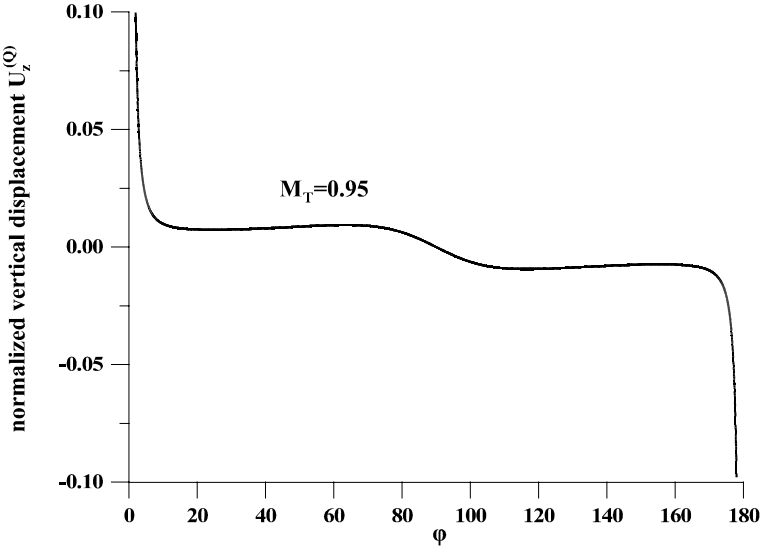

Fig. 18. Variation of the normalized vertical displacement $U_z^{(Q)} = u_z^{(Q)}(1+\varepsilon)^{1/2} r/\kappa Q h$, due to a thermal moving load, with the polar angle φ for $M_T = 0.95$.

sub-Rayleigh range. Finally, Fig. 22 shows the variation of the normalized tangential displacement $U_\varphi^{(Q)}$ with φ for the source velocities $M_T = 0.8$ and 0.95. In the latter case, one may observe the Cauchy-type singularity of $U_\varphi^{(Q)}$ along the Rayleigh Mach wavefronts at $\varphi = 106.47°$.

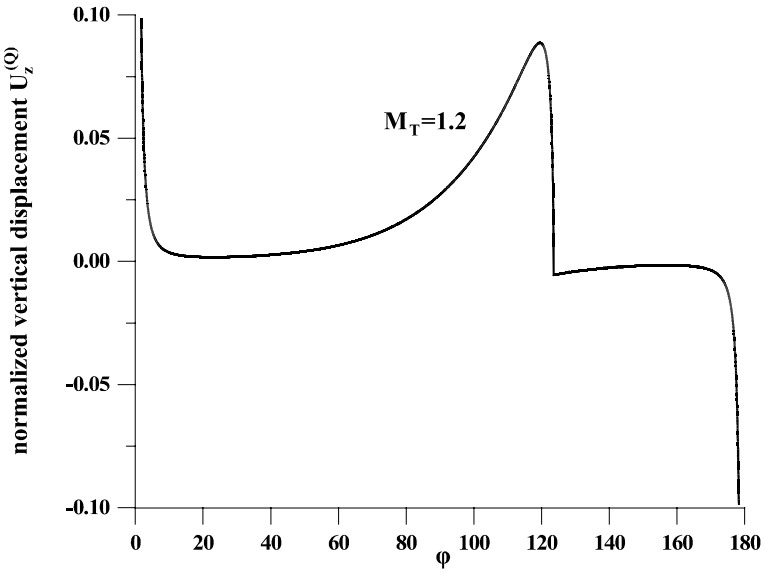

Fig. 19. Variation of the normalized vertical displacement $U_z^{(Q)} = u_z^{(Q)}(1+\varepsilon)^{1/2} r/\kappa Q h$, due to a thermal moving load, with the polar angle φ for $M_T = 1.2$.

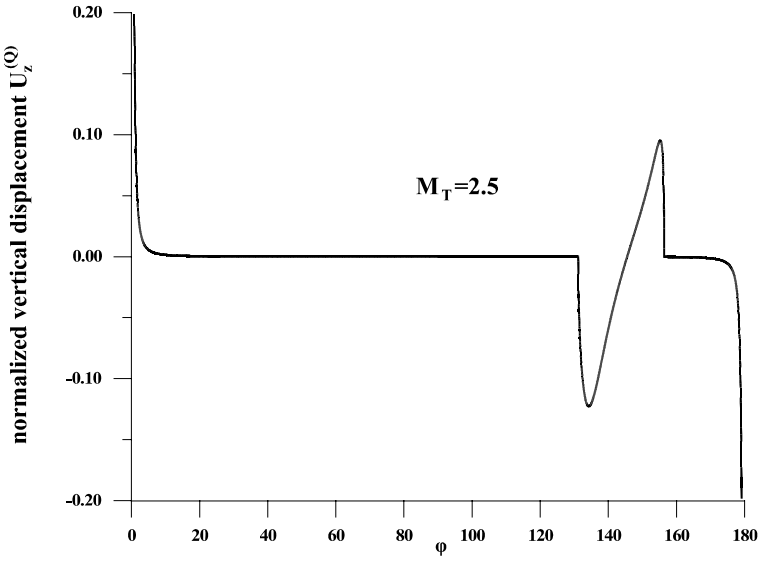

Fig. 20. Variation of the normalized vertical displacement $U_z^{(Q)} = u_z^{(Q)}(1+\varepsilon)^{1/2} r/\kappa Q h$, due to a thermal moving load, with the polar angle φ for $M_T = 2.5$.

10. Concluding remarks

In conclusion, the 3D steady-state dynamical problem of a thermoelastic half space under the action of thermal and mechanical moving sources is treated in this paper. This problem is relevant to model contacts

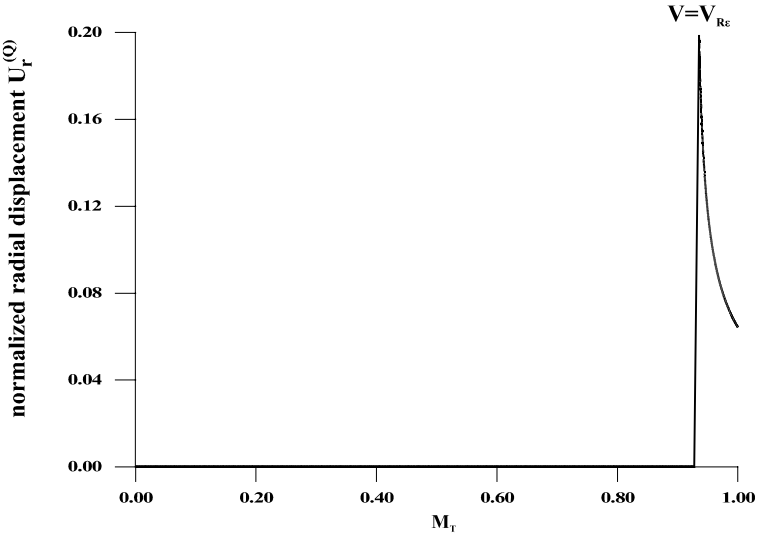

Fig. 21. Variation of the normalized radial displacement $U_r^{(Q)} = u_r^{(Q)}(1+\varepsilon)^{1/2} r/\kappa Q h$, due to a thermal moving load, with the transverse Mach number M_T.

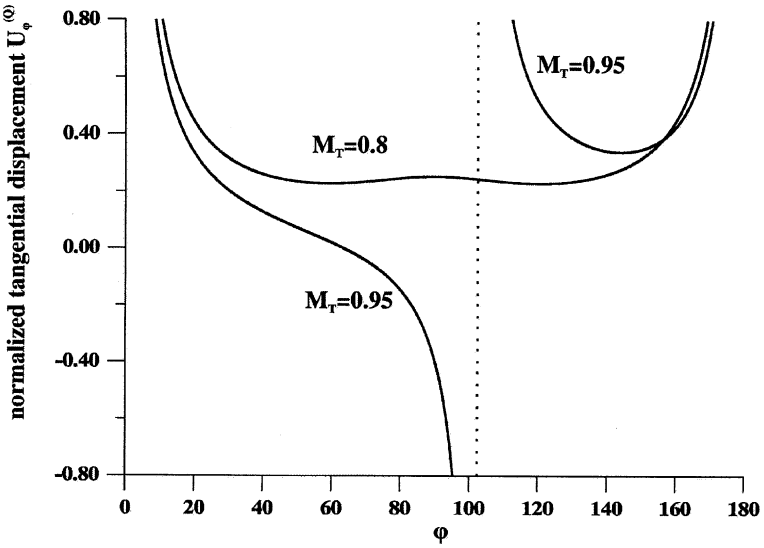

Fig. 22. Variation of the normalized tangential displacement $U_\varphi^{(Q)} = u_\varphi^{(Q)}(1+\varepsilon)^{1/2} r/\kappa Q h$, due to a thermal moving load, with the polar angle φ for $M_T = 0.8$ and 0.95.

of rapidly sliding bodies. Exact solutions are obtained by using a technique based on the Radon transform and distribution theory. The present work completes recent 2D studies (Brock and Georgiadis, 1997, 1999) on the subject of thermo-elastodynamic fundamental solutions of moving-load problems since it deals with the more difficult and more interesting 3D problem. The present results can also be used as Green's functions for *integral-equation* solutions of more general 3D elastodynamic contact problems.

Appendix A

Following a relative idea from Rahman and Barber (1995), who considered the 'pure elastic' Rayleigh function, we write the thermoelastic function $K_\varepsilon(M_T,\varepsilon)$ defined in Eq. (32) of the main text of the paper in the form

$$\begin{aligned} K_\varepsilon(M_T,\varepsilon) &= M_T^2\{M_T^6 - 8M_T^4 + 8(3-2m_\varepsilon^{-2})M_T^2 - 16(1-m_\varepsilon^{-2})\} \\ &= M_T^2(M_T^2 - m_{1\varepsilon})(M_T^2 - m_{2\varepsilon})(M_T^2 - m_{3\varepsilon}), \end{aligned} \tag{A.1}$$

where $(m_{1\varepsilon}, m_{2\varepsilon}, m_{3\varepsilon})$ are the non-trivial zeroes of $K(M_T,\varepsilon)$. The following analytic expressions for these zeroes can be obtained

$$m_{1\varepsilon} = \frac{4}{3}\left[2 + \frac{2^{1/3}(5v_\varepsilon - 2)}{\beta(v_\varepsilon)} - \frac{2^{2/3}}{4(1-v_\varepsilon)}\beta(v_\varepsilon)\right], \tag{A.2}$$

$$m_{2\varepsilon} = \frac{2}{3}\left[4 - \frac{2^{1/3}(1+\mathrm{i}3^{1/2})(5v_\varepsilon - 2)}{\beta(v_\varepsilon)} + \frac{2^{2/3}(1-\mathrm{i}3^{1/2})}{4(1-v_\varepsilon)}\beta(v_\varepsilon)\right], \tag{A.3}$$

$$m_{3\varepsilon} = \frac{2}{3}\left[4 - \frac{2^{1/3}(1-\mathrm{i}3^{1/2})(5v_\varepsilon - 2)}{\beta(v_\varepsilon)} + \frac{2^{2/3}(1+\mathrm{i}3^{1/2})}{4(1-v_\varepsilon)}\beta(v_\varepsilon)\right], \tag{A.4}$$

where $v_\varepsilon = [v + \varepsilon(1-v)]/[1 + 2\varepsilon(1-v)]$ is a material constant that depends upon the Poisson ratio and the coupling constant of the material, $\mathrm{i} = (-1)^{1/2}$, $\beta(v_\varepsilon) = [3^{3/2}\gamma(v_\varepsilon) + 56v_\varepsilon^3 - 123v_\varepsilon^2 + 78v_\varepsilon - 11]^{1/3}$, and $\gamma(v_\varepsilon) = [(1-v_\varepsilon)^3(32v_\varepsilon^3 - 16v_\varepsilon^2 + 21v_\varepsilon - 5)]^{1/2}$.

Further, an inspection on the above functions and a graphical representation of the functions $m_{1\varepsilon}(v_\varepsilon)$, $\mathrm{Re}(m_{2\varepsilon}(v_\varepsilon))$, $\mathrm{Re}(m_{3\varepsilon}(v_\varepsilon))$, $(m_{2\varepsilon} - m_\varepsilon^2)$ and $(m_{3\varepsilon} - m_\varepsilon^2)$, where $\mathrm{Re}(\ )$ denotes the real part of a complex function and $m_\varepsilon = [2(1-v_\varepsilon)/(1-2v_\varepsilon)]^{1/2}$, reveal the following points: (i) The zero $m_{1\varepsilon}$ is real for all values of v_ε and coincides with the non-trivial zero of the Rayleigh function $R_\varepsilon(M_T,\varepsilon)$. (ii) The zeros $m_{2\varepsilon}$ and $m_{3\varepsilon}$ are also zeros of the function $(2 - M_T^2)^2 + 4(1 - M_{L\varepsilon}^2)^{1/2}(1 - M_T^2)^{1/2}$. They are real in the interval $0 < v_\varepsilon \leqslant v_0$, where $v_0 = 0.26308206488336365\ldots$, and complex conjugate in the interval $v_0 < v_\varepsilon < 0.5$. We also notice that v_0 is the real zero of $\gamma(v_\varepsilon)$. (iii) The inequalities $m_{1\varepsilon} < 1 < \mathrm{Re}(m_{2\varepsilon}) < \mathrm{Re}(m_{3\varepsilon})$ are valid. (iv) The inequalities $M_{L\varepsilon}^2 < M_T^2 \leqslant m_\varepsilon^2 < m_{2\varepsilon} < m_{3\varepsilon}$ are valid in the subsonic and transonic speed ranges if $(m_{2\varepsilon}, m_{3\varepsilon})$ are real (i.e. in the interval $0 < v_\varepsilon \leqslant v_0$). (v) The equality $m_{1\varepsilon}m_{2\varepsilon}m_{3\varepsilon} = 16(1 - m_\varepsilon^{-2})$ is always valid.

Having available, through (A.1), the factorization forms of K_ε and R_ε permits writing (64) and other analogous equations in the main text of the paper.

Finally, the expansions of the functions (A, B, C, D, E, N) in sums of partial fractions are as follows:

$$A(M_T,\varepsilon) = \frac{4(1 - M_{L\varepsilon}^2)}{\prod_{j=1}^3 (M_T^2 - m_{j\varepsilon})} = \sum_{j=1}^3 \frac{A_j}{(M_T^2 - m_{j\varepsilon})}, \tag{A.5}$$

$$B(M_T,\varepsilon) = \frac{(2 - M_T^2)^3}{\prod_{j=1}^3 (M_T^2 - m_{j\varepsilon})} = \sum_{j=1}^3 \frac{B_j}{(M_T^2 - m_{j\varepsilon})}, \tag{A.6}$$

$$C(M_T,\varepsilon) = \frac{(8m_\varepsilon^{-2} - 4) + (6 - 8m_\varepsilon^{-2})M_T^2 - M_T^4}{\prod_{j=1}^3 (M_T^2 - m_{j\varepsilon})} = \sum_{j=1}^3 \frac{C_j}{(M_T^2 - m_{j\varepsilon})}, \tag{A.7}$$

$$D(M_{\mathrm{T}},\varepsilon)=\frac{2(2-M_{\mathrm{T}}^2)}{\prod_{j=1}^{3}(M_{\mathrm{T}}^2-m_{j\varepsilon})}=\sum_{j=1}^{3}\frac{D_j}{(M_{\mathrm{T}}^2-m_{j\varepsilon})}, \tag{A.8}$$

$$E(M_{\mathrm{T}},\varepsilon)=\frac{(2-M_{\mathrm{T}}^2)^3}{\prod_{j=0}^{3}(M_{\mathrm{T}}^2-m_{j\varepsilon})}=\sum_{j=0}^{3}\frac{E_j}{(M_{\mathrm{T}}^2-m_{j\varepsilon})}, \tag{A.9}$$

$$N(M_{\mathrm{T}},\varepsilon)=\frac{4(2-M_{\mathrm{T}}^2)}{\prod_{j=0}^{3}(M_{\mathrm{T}}^2-m_{j\varepsilon})}=\sum_{j=0}^{3}\frac{N_j}{(M_{\mathrm{T}}^2-m_{j\varepsilon})}, \tag{A.10}$$

where $m_{0\varepsilon}\equiv 0$ and

$$A_1=\frac{4(1-m_\varepsilon^{-2}m_{1\varepsilon})}{(m_{1\varepsilon}-m_{2\varepsilon})(m_{1\varepsilon}-m_{3\varepsilon})},\qquad A_2=\frac{4(1-m_\varepsilon^{-2}m_{2\varepsilon})}{(m_{2\varepsilon}-m_{1\varepsilon})(m_{2\varepsilon}-m_{3\varepsilon})},$$
$$A_3=\frac{4(1-m_\varepsilon^{-2}m_{3\varepsilon})}{(m_{3\varepsilon}-m_{1\varepsilon})(m_{3\varepsilon}-m_{2\varepsilon})}, \tag{A.11a–c}$$

$$B_1=\frac{(2-m_{1\varepsilon})^2}{(m_{1\varepsilon}-m_{2\varepsilon})(m_{1\varepsilon}-m_{3\varepsilon})},\quad B_2=\frac{(2-m_{2\varepsilon})^2}{(m_{2\varepsilon}-m_{1\varepsilon})(m_{2\varepsilon}-m_{3\varepsilon})},\quad B_3=\frac{(2-m_{3\varepsilon})^2}{(m_{3\varepsilon}-m_{1\varepsilon})(m_{3\varepsilon}-m_{2\varepsilon})}, \tag{A.12a–c}$$

$$C_1=\frac{(8m_\varepsilon^{-2}-4)+(6-8m_\varepsilon^{-2})m_{1\varepsilon}-m_{1\varepsilon}^2}{(m_{1\varepsilon}-m_{2\varepsilon})(m_{1\varepsilon}-m_{3\varepsilon})},\qquad C_2=\frac{(8m_\varepsilon^{-2}-4)+(6-8m_\varepsilon^{-2})m_{2\varepsilon}-m_{2\varepsilon}^2}{(m_{2\varepsilon}-m_{1\varepsilon})(m_{2\varepsilon}-m_{3\varepsilon})},$$
$$C_3=\frac{(8m_\varepsilon^{-2}-4)+(6-8m_\varepsilon^{-2})m_{3\varepsilon}-m_{3\varepsilon}^2}{(m_{3\varepsilon}-m_{1\varepsilon})(m_{3\varepsilon}-m_{2\varepsilon})}, \tag{A.13a–c}$$

$$D_1=\frac{2(2-m_{1\varepsilon})}{(m_{1\varepsilon}-m_{2\varepsilon})(m_{1\varepsilon}-m_{3\varepsilon})},\qquad D_2=\frac{2(2-m_{2\varepsilon})}{(m_{2\varepsilon}-m_{1\varepsilon})(m_{2\varepsilon}-m_{3\varepsilon})},$$
$$D_3=\frac{2(2-m_{3\varepsilon})}{(m_{3\varepsilon}-m_{1\varepsilon})(m_{3\varepsilon}-m_{2\varepsilon})}, \tag{A.14a–c}$$

$$E_0=-\frac{8}{m_{1\varepsilon}m_{2\varepsilon}m_{3\varepsilon}},\qquad E_1=\frac{(2-m_{1\varepsilon})^3}{m_{1\varepsilon}(m_{1\varepsilon}-m_{2\varepsilon})(m_{1\varepsilon}-m_{3\varepsilon})},$$
$$E_2=\frac{(2-m_{2\varepsilon})^3}{m_{2\varepsilon}(m_{2\varepsilon}-m_{1\varepsilon})(m_{2\varepsilon}-m_{3\varepsilon})},\quad E_3=\frac{(2-m_{3\varepsilon})^3}{m_{3\varepsilon}(m_{3\varepsilon}-m_{1\varepsilon})(m_{3\varepsilon}-m_{2\varepsilon})}, \tag{A.15a–d}$$

$$N_0=-\frac{8}{m_{1\varepsilon}m_{2\varepsilon}m_{3\varepsilon}},\qquad N_1=\frac{4(2-m_{1\varepsilon})}{m_{1\varepsilon}(m_{1\varepsilon}-m_{2\varepsilon})(m_{1\varepsilon}-m_{3\varepsilon})},$$
$$N_2=\frac{4(2-m_{2\varepsilon})}{m_{2\varepsilon}(m_{2\varepsilon}-m_{1\varepsilon})(m_{2\varepsilon}-m_{3\varepsilon})},\quad N_3=\frac{4(2-m_{3\varepsilon})}{m_{3\varepsilon}(m_{3\varepsilon}-m_{1\varepsilon})(m_{3\varepsilon}-m_{2\varepsilon})}. \tag{A.16a–d}$$

References

Atkinson, C., Craster, R.V., 1992. Fracture in fully coupled dynamic thermoelasticity. J. Mech. Phys. Solids 40, 1415–1432.
Barber, J.R., 1984. Thermoelastic displacements and stresses due to a heat source moving over the surface of a half plane. ASME J. Appl. Mech. 51, 636–640.

Barber, J.R., 1996. Surface displacements due to a steadily moving point force. ASME J. Appl. Mech. 63, 245–251.
Barber, J.R., Ciavarella, M., 2000. Contact mechanics. Int. J. Solids Struct. 37, 29–43.
Biot, M.A., 1956. Thermoelasticity and irreversible thermodynamics. J. Appl. Phys. 27, 240–253.
Brock, L.M., 1995. Slip/diffusion zone formation at rapidly-loaded cracks in thermoelastic solids. J. Elasticity 40, 183–206.
Brock, L.M., 1997. Transient three-dimensional Rayleigh and Stoneley signal effects in thermoelastic solids. Int. J. Solids Struct. 34, 1463–1478.
Brock, L.M., Georgiadis, H.G., 1997. Steady-state motion of a line mechanical / heat source over a half-space: A thermoelastodynamic solution. ASME J. Appl. Mech. 64, 562–567.
Brock, L.M., Georgiadis, H.G., 1999. Convection effects for rapidly moving mechanical sources on a half-space governed by fully coupled thermoelasticity. ASME J. Appl. Mech. 66, 347–351.
Brock, L.M., Georgiadis, H.G., 2000. Sliding contact with friction of a thermoelastic solid at subsonic, transonic and supersonic speeds. J. Thermal Stresses 23, 629–656.
Brock, L.M., Georgiadis, H.G., Tsamasphyros, G., 1997. The coupled thermoelasticity problem of the transient motion of a line heat/mechanical source over a half-space. J. Thermal Stresses 20, 773–795.
Brock, L.M., Rodgers, M.J., 1997. Steady-state response of a thermoelastic half-space to the rapid motion of surface thermal/mechanical loads. J. Elasticity 47, 225–240.
Bryant, M.D., 1988. Thermoelastic solutions for thermal distributions moving over half space surfaces and application to the moving heat source. ASME J. Appl. Mech. 55, 87–92.
Carlson, D.E., 1972. Linear thermoelasticity. In: Flugge, S. (Ed.), Handbuch der Physik, vol. VIa/2. Springer, Berlin, pp. 297–345.
Chadwick, P., 1960. Thermoelasticity: The dynamical theory. In: Sneddon, I.N., Hill, R. (Eds.), Progress in Solid Mechanics, vol. 1. North-Holland, Amsterdam, pp. 263–328.
Dassios, G., Grillakis, M., 1984. Dissipation rates and partition of energy in thermoelasticity. Arch. Rational Mech. Anal. 87, 49–91.
Deans, S.R., 1983. The Radon Transform and Some of Its Applications. John Wiley & Sons Inc, New York.
Eason, G., 1965. The stresses produced in semi-infinite solid by a moving surface force. Int. J. Engng. Sci. 2, 581–609.
Fung, Y.C., 1965. Foundations of Solid Mechanics. Prentice-Hall, Englewood Cliffs, NJ.
Gel'fand, I.M., Shilov, G.E., 1964. In: Generalized Functions, vol. 1. Academic Press, New York.
Gel'fand, I.M., Graev, M.I., Vilenkin, N.Ya., 1966. In: Generalized Functions, vol. 5. Academic Press, New York.
Georgiadis, H.G., 1986. On the stress singularity in steady-state transonic shear crack propagation. Int. J. Fract. 30,, 175–180.
Georgiadis, H.G., Barber, J.R., 1993. On the super-Rayleigh/subseismic elastodynamic indentation problem. J. Elasticity 31, 141–161.
Georgiadis, H.G., Brock, L.M., Rigatos, A.P., 1998. Transient concentrated thermal/mechanical loading of the faces of a crack in a coupled-thermoelastic solid. Int. J. Solids Struct. 35, 1075–1097.
Georgiadis, H.G., Lykotrafitis, G., 2001. A method based on the Radon transform for three-dimensional elastodynamic problems of moving loads. J. Elasticity 65, 87–129.
Georgiadis, H.G., Rigatos, A.P., Brock, L.M., 1999. Thermoelastodynamic disturbances in a half-space under the action of a buried thermal/mechanical line source. Int. J. Solids Struct. 36, 3639–3660.
Hoskins, R.F., 1979. Generalized Functions. Ellis Horwood Ltd, Chichester.
Huang, J.H., Ju, F.D., 1985. Thermomechanical cracking due to moving frictional loads. Wear 102, 81–104.
Huang, Y., Wang, W., Liu, C., Rosakis, A.J., 1998. Intersonic crack growth in bimaterial interfaces: An investigation of crack face contact. J. Mech. Phys. Solids 46, 2233–2259.
Jahanshahi, A., 1966. Quasi-static stresses due to moving temperature discontinuity on a plane boundary. ASME J. Appl. Mech. 33, 814–816.
Ju, F.D., Huang, J.H., 1982. Heat checking in the contact zone of a bearing seal: A two-dimensional model of a single moving asperity. Wear 79, 107–118.
Kanwal, R.P., 1998. Generalized Functions: Theory and Technique. Birkhäuser, Boston.
Kennedy, F.D., 1984. Thermal and thermomechanical effects in dry sliding. Wear 100, 453–476.
Kilaparti, S.R., Burton, R.A., 1978. The thermoelastic patch contact problem for large Peclet number. ASME J. Lubr. Technol. 100, 65–69.
Krylov, V.V., Dawson, A.R., Heelis, M.E., Collop, A.C., 2000. Rail movement and ground waves caused by high-speed trains approaching track-soil critical velocities. Proc. Inst. Mech. Engrs. (Part F) 214, 107–116.
Lansing, D.L., 1966. The displacement in an elastic half-space due to a moving concentrated normal load. NASA Technical Report R-238.
Lauwerier, H.A., 1963. The Hilbert problem for generalized functions. Arch. Rational Mech. Anal. 13, 157–166.
Lefeuvemesgouez, G., Lehouedec, D., Peplow, A.T., 2000. Ground vibration in the vicinity of a high-speed moving harmonic strip load. J. Sound Vibr. 231, 1289–1309.

Ling, F.F., Mow, V.C., 1965. Surface displacements of a convective elastic half-space under an arbitrarily distributed fast-moving heat source. ASME J. Basic Engng. 87, 729–734.
Ling, F.F., Ng, C.W., 1962. On temperatures at the interfaces of bodies in sliding contact. In: Proc. 4th U.S. National Congress Appl. Mech.. ASME, New York, pp. 1343–1349.
Ludwig, D., 1966. The Radon transform on Euclidean space. Commun. Pure Appl. Math. 19, 49–81.
Massalas, C.V., Anagnostaki, E., Kalpakidis, V.K., 1985. Some considerations on the coupled thermoelastic problems. Lett. Appl. Engng. Sci. 23 (6), 677–683.
Mow, V.C., Cheng, H.S., 1967. Thermal stresses in an elastic half space associated with an arbitrarily distributed moving heat source. J. Appl. Math. Phys. (ZAMP) 18, 500–507.
Poruchikov, V.B., 1993. Methods of the Classical Theory of Elastodynamics. Springer-Verlag, Berlin.
Rahman, M., Barber, J.R., 1995. Exact expressions for the roots of the secular equation for Rayleigh waves. ASME J. Appl. Mech. 62, 250–252.
Roos, B.W., 1969. Analytic Functions and Distributions in Physics and Engineering. Wiley, New York.
Rosakis, A.J., Samudrala, O., Singh, R.P., Shukla, A., 1998. Intersonic crack propagation in bimaterial systems. J. Mech. Phys. Solids 46, 1789–1813.
Shmegera, S.V., 2000. The initial boundary-value mixed problems for elastic half-plane with the conditions of contact friction. Int. J. Solids Struct. 37, 6277–6296.
Sveklo, V.A., 1964. Boussinesq type problems for the anisotropic half-space. J. Appl. Math. Mech. (PMM) 28, 1099–1105.
Wang, C.-Y., Achenbach, J.D., 1996. Lamb's problem for solids of general anisotropy. Wave Motion 24, 227–242.
Willis, J.R., 1966. Hertzian contact of anisotropic bodies. J. Mech. Phys. Solids 14, 163–176.
Willis, J.R., 1970. The distribution of stress in an anisotropic elastic body containing an exterior crack. Int. J. Engng. Sci. 8, 559–574.
Willis, J.R., 1973. Self-similar problems in elastodynamics. Phil. Trans. Royal Soc. (London) 274, 435–471.